

# Safe Active Dynamics Learning and Control: A Sequential Exploration-Exploitation Framework

Thomas Lew, Apoorva Sharma, James Harrison, Andrew Bylard, and Marco Pavone

**Abstract**—Safe deployment of autonomous robots in diverse scenarios requires agents that are capable of efficiently adapting to new environments while satisfying constraints. In this work, we propose a practical and theoretically-justified approach to maintaining safety in the presence of dynamics uncertainty. Our approach leverages Bayesian meta-learning with last-layer adaptation: the expressiveness of neural-network features trained offline, paired with efficient last-layer online adaptation, enables the derivation of tight confidence sets which contract around the true dynamics as the model adapts online. We exploit these confidence sets to plan trajectories that guarantee the safety of the system. Our approach handles problems with high dynamics uncertainty where reaching the goal safely is initially infeasible by first *exploring* to gather data and reduce uncertainty, before autonomously *exploiting* the acquired information to safely perform the task. Under reasonable assumptions, we prove that our framework has high-probability guarantees of satisfying all constraints at all times jointly. This analysis also motivates two regularizers of last-layer meta-learners that improve online adaptation capabilities as well as performance by reducing the size of the confidence sets. We extensively demonstrate our approach in simulation and on hardware.

Hardware results are available at [youtu.be/bvG-g3NADUc](https://youtu.be/bvG-g3NADUc).

**Index Terms**—Robotics, meta-learning, chance-constrained optimization, planning, control, system identification, dynamics, reachability analysis.

## I. INTRODUCTION

Deploying truly autonomous robotic systems in safety-critical applications requires agents that are capable of adapting to new environments while satisfying constraints. For example, an autonomous robot assisting astronauts in space must be able to handle a priori unknown payloads while respecting velocity constraints and avoiding collisions with obstacles. This requires quantifying the uncertainty in the environment and factoring it into the decision process to take reliable actions. As the initial levels of uncertainty may be very high as the agent encounters a new environment, this also requires choosing actions that actively reduce the level of uncertainty to eventually be capable to safely perform the given task. For instance, a robot grasping a new payload should first identify the properties of its coupled dynamics before attempting to transport its cargo to a destination.

Despite recent rapid progress on facets of this problem in the fields of data-driven control, machine learning, and reinforcement learning, the overall problem of safely controlling a robotic system in uncertain environments remains a challenge. Specifically, it is difficult to (1) obtain statistical models which

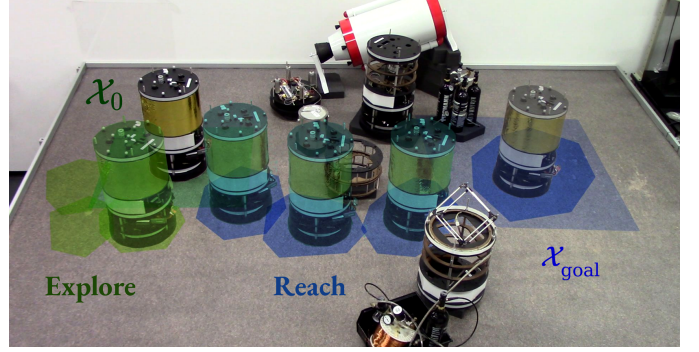


Fig. 1. We propose a learning-based control framework to tackle problems where uncertainty over a system’s dynamics is initially too high to safely perform the given task (e.g., transporting an uncertain payload). By leveraging meta-learning and (full-horizon) reachability-aware chance-constrained optimal control, our algorithm actively *explores* to infer dynamics and reduce uncertainty, until it is possible to safely *reach* the goal. We prove that our framework guarantees with high probability the satisfaction of all constraints at all times jointly, even if performing the task is impossible even with perfect information, e.g., if the only path to the goal is blocked by an obstacle.

are general yet offer a tight characterization of uncertainty, (2) design control laws that formally guarantee the safety of uncertain nonlinear dynamical systems, and (3) ensure that these guarantees hold even as the system adapts and reduces uncertainty using online data. Designing a robotic system that is capable of actively and safely exploring its environment without human intervention remains an open challenge.

**Contributions:** We propose a practical framework for the safe learning and control of uncertain nonlinear systems. Specifically, our approach is capable of tackling chance-constrained problems that are initially infeasible due to high dynamics uncertainty by autonomously exploring and learning online to reduce uncertainty before performing the task. This framework is enabled by the following contributions:

- *Dynamics modeling:* We show that last-layer meta-learning models can learn tight and structured representations of uncertain dynamics from data and can efficiently reduce uncertainty online. Critically, we derive adaption guarantees of such models in the form of confidence sets guaranteed with high probability to contain the true dynamics throughout the online learning process. These guarantees rely on two realistic and intuitive assumptions on the quality of the *offline* meta-training process which can be empirically validated before deploying the system. This theoretical analysis also suggests two regularizers for offline meta-training yielding improved performance and a more expressive model class for online adaptation.

The authors are with the Department of Aeronautics & Astronautics, Stanford University, Stanford, CA 94305-4035 USA (emails: {thomas.lew, apoorva, jharrison, bylard, pavone}@stanford.edu).

- *Autonomous exploration*: We combine these confidence sets with reachability-aware trajectory optimization to tackle problems with high levels of uncertainty that are initially infeasible. Specifically, we use the current level of uncertainty to autonomously switch from active learning to reduce dynamics uncertainty (the exploration phase) to execution of the desired task (the exploitation phase) once the task becomes feasible.
- *Safety*: In this work, we define safety in terms of the satisfaction of all constraints over the entire operation time. As such, we prove that our framework guarantees, with high probability, the satisfaction of all constraints *jointly*, i.e. over the total task duration. This contrasts with prior work which enforces pointwise chance constraints instead (see Section II). We also prove that the algorithm is continually recursively feasible with high probability, which is crucial to enable autonomous operation. Our guarantees are independent of the (unknown) total time required to solve the task, and safety still holds even if the perfect-information problem is impossible to solve, e.g., if the only path to the goal is blocked by an obstacle.

We validate our approach on two challenging highly uncertain nonlinear systems and show that we are able to autonomously and safely infer dynamics to accomplish goal-reaching tasks. We also provide hardware experiments demonstrating the reliability and real-time capabilities of our approach, as well as the practical applicability of dynamics meta-learning models with last-layer adaptation.

**Organization:** We first discuss related work in Section II. Section III describes our chance-constrained problem formulation. We present our contributions to the meta-learning model used to capture uncertain dynamics in Section IV and our control approach in Section V. Finally, we present results in Sections VI and VII and conclude in Section VIII.

**Notation:**  $\chi_d^2(p)$  denotes the  $p$ -th quantile of the  $\chi^2$  distribution with  $d$  degrees of freedom. For any  $\mathbf{a}, \mathbf{b} \in \mathbb{R}^d$ , and  $\mathbf{A}$  a  $d \times d$  positive definite matrix, define  $\|\mathbf{a}\|_{\mathbf{A}}^2 = \mathbf{a}^T \mathbf{A} \mathbf{a}$ , and  $\bar{\lambda}(\mathbf{A})$  (and  $\underline{\lambda}(\mathbf{A})$ ) for the maximum (and minimum) eigenvalue of  $\mathbf{A}$ .  $\langle \mathbf{a}, \mathbf{b} \rangle$  denotes the inner product of  $\mathbf{a}$  with  $\mathbf{b}$  (for  $\mathbf{a}, \mathbf{b} \in \mathbb{R}^d$ ,  $\langle \mathbf{a}, \mathbf{b} \rangle = \mathbf{a}^T \mathbf{b}$ ).

## II. RELATED WORK

Our approach is enabled by two key components: a dynamics meta-learning model with adaptation guarantees and a sequential exploration and exploitation control algorithm.

**Choosing a model:** In contrast to model-free approaches to learning-based control, model-based methods generally provide better sample efficiency while enabling guarantees on constraint satisfaction and stability [1], [2]. These model-based methods rely on the choice of a dynamics model—e.g., neural networks [3], squared-exponential kernel Gaussian processes [2], or linear models [4]—each with associated strengths and weaknesses. Recent work in the controls community has leveraged behavioral systems theory to guarantee stability and probabilistic constraint satisfaction of a non-parametric MPC scheme [5]–[7]. Although such methods have been shown to perform well for nonlinear systems [4], their guarantees

currently do not extend beyond linear systems. Alternatively, assuming linearly parameterizable dynamics with known nonlinear basis functions allows the design of stable adaptive controllers [8], [9] and planning algorithms with adaptation guarantees [10], [11]. When such structure is not known a priori, purely data-driven models such as neural networks can be used to derive nonlinear controllers that guarantee stability [12]. However, these methods require collecting a dataset characterizing the system dynamics throughout the operational regime and would need retraining with a new dataset if the environment or the system change, which is prohibitively expensive in terms of data requirements.

To tackle problems where data is scarce, meta-learning [13]–[15] aims to train a model from data over different tasks that is capable of rapid adaptation given limited data from a given task. In the context of dynamics learning, a task corresponds to a dynamical system and meta-learning consists of training a model capable of efficiently fitting the true system’s dynamics with limited data. Prior work has successfully applied meta-learning to learning-based control [15]–[17]: performing gradient descent on meta-learned neural networks at run-time enables fast adaptation with limited data. However, the non-convexity of the online adaptation objective makes it difficult to provide adaptation guarantees for such gradient descent approaches.

Instead, our approach obtains the best of both worlds by combining meta-trained neural network features with online last layer adaptation [18]: offline, data from related environments is used to train a neural network to produce features tailored to the structure of the system; online, only adapting the last layer yields a sample-efficient adaptation process with strong guarantees on statistical performance. By taking a Bayesian perspective on meta-learning, our model also yields a calibrated prior uncertainty representation that enables quantifying the initial uncertainty of the system. Importantly, building on this initial uncertainty quantification, the linear structure of the last layer adaptation process enables constructing confidence sets for the parameters of the model that hold throughout the online learning process.

Within the realm of Bayesian modeling, another common modeling choice is Gaussian processes (GPs) [19]. GPs with squared-exponential kernels have been widely used to represent dynamics for learning-based control and exploration, as they can represent any bounded continuous function arbitrarily well given enough data. While bounds providing similar guarantees as our confidence sets can be derived for these models, such bounds are generally too conservative [20] so that scaling constants are heuristically selected in experiments [21], [22]. Alternatively, it is common to assume that the true system dynamics lie in an RKHS determined by finite-dimensional basis functions [10], [11]. Importantly, this approach enables deriving tighter bounds over possible models [23] which we regularize for and use directly in this work. In contrast to prior work, we explicitly learn these basis functions and regularize these features to improve generalization of the model. Moreover, we quantify prior uncertainty in an offline meta-training procedure, creating a model which is both calibrated and expressive enough to represent possible systems. This also

allows verifying that representation error is small *offline* before deploying the system.

**Safe dynamics learning and control** amounts to the design of a controller that guarantees satisfaction of all constraints. Given a statistical model of the system subject to external random disturbances, it is common to use chance constraints to ensure that all specifications are satisfied with high probability  $1-\delta$ . Such chance constraints are often preferred to robust constraints ( $\delta=0$ ), as statistical models predicting unbounded distributions over possible outcomes are typically used in such applications [24]–[26], in which case requiring zero probability of failure is infeasible. Typically, *pointwise* chance constraints taking the form  $\mathbb{P}(\mathbf{x}_t \in \mathcal{X}_i) \geq (1-\delta)$  are enforced for each  $i$ -th constraint  $\mathbf{x}_t \in \mathcal{X}_i$  at each time  $t \geq 0$  [24], [26]–[30]. Unfortunately, this approach only guarantees constraint satisfaction with high probability at each timestep  $t$ , and does not guarantee safety over the entire operation time [31], [32]. This is particularly an issue when the time to complete a given task is a priori unknown. This observation motivates using a single *joint* chance constraint instead, taking the form  $\mathbb{P}(\mathbf{x}_t \in \mathcal{X}_i \forall i \forall t) \geq (1-\delta)$ . Instead of allocating the total allowed probability of failure  $\delta$  to each  $i$ -th constraint and each time  $t$  [33], we take a frequentist viewpoint and use the confidence sets over the model parameters to plan robust trajectories that are safe with respect to all possible parameters in these confidence sets. This approach is key to guaranteeing the satisfaction of all constraints at all times with probability at least  $(1-\delta)$  despite an unknown time to complete the task and while switching between exploration to reduce dynamics uncertainty and exploitation to complete the given task.

Reinforcement learning (RL) can also be effective for controlling uncertain systems [3], [34] and model-based methods in particular enable an agent to consider its uncertainty over dynamics when choosing actions [2]. However, standard model-based reinforcement learning (MBRL) methods do not provide sufficient guarantees for maintaining safety during operation as they commonly penalize constraint violation [34], whereas safety-aware RL typically considers finite-dimensional state-action spaces, as using continuous state-action spaces remains an open area of research [35], [36]. In contrast to traditional RL, we meta-learn a model and uncertainty representation *offline*, fine-tune it *online* via last-layer adaptation only, and use trajectory optimization and reachability analysis for planning and control. This structure allows our framework to rapidly infer an accurate dynamics model while providing strong safety guarantees throughout the control task.

Our model-based active dynamics learning framework first appeared in [37], which did not provide guarantees of safety. Subsequently, [38] developed a similar trajectory optimization approach to learn dynamics. This approach makes an approximation that neglects the time correlations of parameters uncertainty which impacts the soundness of their theoretical analysis and algorithmic design; these issues are discussed in [39]. Learning-based control algorithms typically tackle the problems of stabilization around an operating point, planning to a goal, active system identification [40], [41], and dual control [10], [11], [42], [43]. These approaches out-perform methods

that neither consider uncertainty nor leverage learning-based components. Still, they rely on the assumption that the problem is initially feasible given the current system’s uncertainty characterization (e.g., learning-based MPC requires the first optimization problem to be feasible). In contrast to prior work, we consider the problem of *eventually* performing a task which is initially infeasible with the current information about the system. Actively learning the system’s properties is thus *necessary* to reduce uncertainty before performing the task. Importantly, we explicitly guarantee the satisfaction of all constraints at all times with high probability, even if the problem is truly infeasible even with perfect information.

### III. PROBLEM FORMULATION

The goal of this work is to enable robots to safely navigate from an initial state  $\mathbf{x}(0)$  to a goal region  $\mathcal{X}_{\text{goal}}$  despite highly uncertain dynamics while minimizing a chosen cost metric  $\ell(\cdot)$  (e.g., fuel consumption). We write the state of the agent at time  $t \in \mathbb{N}$  as  $\mathbf{x}_t \in \mathbb{R}^n$  and the control input as  $\mathbf{u}_t \in \mathbb{R}^m$ . The system follows dynamics  $\mathbf{x}_{t+1} = \mathbf{h}(\mathbf{x}_t, \mathbf{u}_t) + \mathbf{g}(\mathbf{x}_t, \mathbf{u}_t, \boldsymbol{\xi}) + \boldsymbol{\epsilon}_t$ , where  $\mathbf{h}$  is known and corresponds to prior knowledge of the system, whereas  $\mathbf{g}$  is unknown, with unobserved parameters  $\boldsymbol{\xi}$  and stochastic disturbances  $\boldsymbol{\epsilon}_k$ . We assume at the beginning of each episode  $j$ , the parameters are sampled  $\boldsymbol{\xi}_j \sim p(\boldsymbol{\xi})$  and are fixed for the episode duration. These parameters correspond to unknown features that vary between episodes such as the mass and inertia of a payload. We assume that the disturbances  $\boldsymbol{\epsilon}_t = (\epsilon_t^1, \dots, \epsilon_t^n)$  are uncorrelated over  $t \in \mathbb{N}$  and  $i = 1, \dots, n$  and that each  $\epsilon_t^i$  is  $\sigma_i$ -subgaussian and bounded such that  $\epsilon_t^i \in \mathcal{E}_i$ , where  $\mathcal{E}_i$  is a bounded subset of  $\mathbb{R}$ .

Critically, this algorithm should ensure that constraints are satisfied *at all times*, avoiding obstacles ( $\mathbf{x}_t \notin \mathcal{X}_{\text{obs}}$ , where  $\mathcal{X}_{\text{obs}}$  is the obstacle set) and respecting system constraints ( $\mathbf{x}_t \in \mathcal{X}$ ,  $\mathbf{u}_t \in \mathcal{U}$ , where  $\mathcal{X}, \mathcal{U}$  are feasible state and control sets). Due to the system stochasticity and uncertain dynamics, strict enforcement of all constraints for all times may be challenging without further assumptions, e.g., bounded model mismatch. Instead, we enforce all constraints via a single chance constraint at probability level  $(1-\delta) \in (0, 1)$ . Specifically, we define a *joint chance constraint* which should hold at all times until the goal  $\mathcal{X}_{\text{goal}}$  is reached. The full problem is expressed as

#### Chance-Constrained Optimal Control Problem (CC-OCPP)

$$\min_{\mathbf{x}, \mathbf{u}} \mathbb{E} \left( \sum_{t=0}^N \ell(\mathbf{x}_t, \mathbf{u}_t) \right) \quad \text{s.t.} \quad \mathbf{x}_0 = \mathbf{x}(0), \quad (1a)$$

$$\mathbf{x}_{t+1} = \mathbf{h}(\mathbf{x}_t, \mathbf{u}_t) + \mathbf{g}(\mathbf{x}_t, \mathbf{u}_t, \boldsymbol{\xi}) + \boldsymbol{\epsilon}_t, \quad t=0, \dots, N-1, \quad (1b)$$

$$\mathbb{P} \left( \bigcap_{t=1}^N \mathbf{x}_t \in \mathcal{X}_{\text{free}} \wedge \bigcap_{t=0}^{N-1} \mathbf{u}_t \in \mathcal{U} \wedge \mathbf{x}_N \in \mathcal{X}_{\text{goal}} \right) \geq 1 - \delta, \quad (1c)$$

where  $\mathbf{x} = (\mathbf{x}_0, \dots, \mathbf{x}_N)$ ,  $\mathbf{u} = (\mathbf{u}_0, \dots, \mathbf{u}_{N-1})$ ,  $\mathcal{X}_{\text{free}} = \mathcal{X} \setminus \mathcal{X}_{\text{obs}}$ ,  $\mathcal{X}_{\text{goal}} \subset \mathcal{X}_{\text{free}}$ , and  $N$  is the total problem duration (possibly infinite). Note that this problem formulation can be equivalently described as a constrained Markov decision process [44] with a continuous state and action space, general nonlinear stochastic dynamics, and a non-convex cost function.

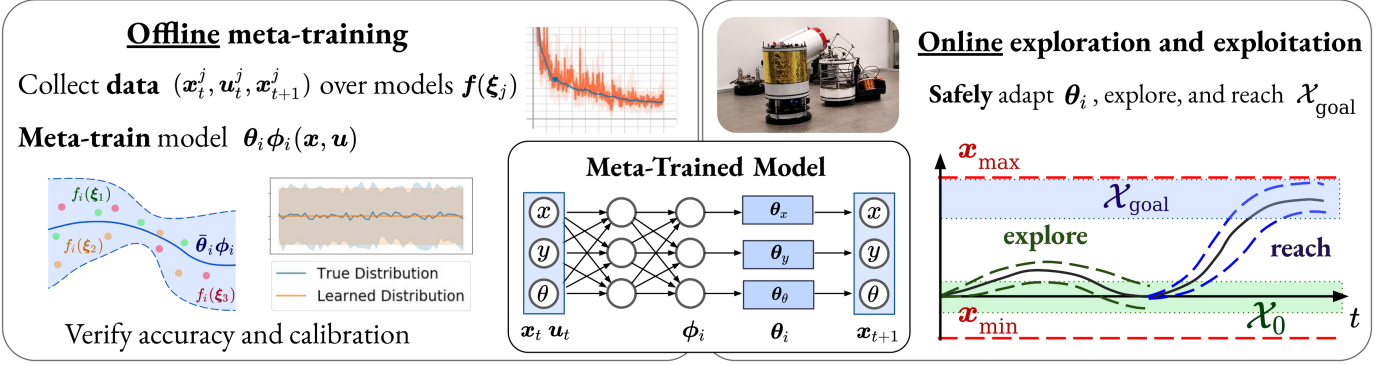


Fig. 2. To guarantee safety at all times and reach a goal region  $\mathcal{X}_{\text{goal}}$  despite uncertain dynamics  $\mathbf{f}$ , our framework consists of an offline phase, where a dataset over multiple models is used to meta-train an uncertain model of the system. Then, it is deployed and safely adapts the last layers  $\theta_i$  of the meta-trained model, autonomously explores the environment to decrease its uncertainty, and safely reaches the goal.

Satisfying safety constraints with unknown dynamics at all times is extremely difficult without further information. Thus, our approach relies on the following assumption [22]:

**Assumption 1 (A1).**  $\mathbf{x}(0) \in \mathcal{X}_0 \subset \mathcal{X}_{\text{free}}$ , where  $\mathcal{X}_0$  is a control invariant set and we have a feedback controller  $\pi(\cdot) : \mathcal{X}_0 \rightarrow \mathcal{U}$  under which it is possible to remain in  $\mathcal{X}_0$  for all  $\xi$  and  $\epsilon$ , i.e.,  $\mathbf{x}_t \in \mathcal{X}_0, \mathbf{u}_t = \pi(\mathbf{x}_t) \implies \mathbf{x}_{t+1} \in \mathcal{X}_0 \forall \xi, \epsilon$ , with  $\mathbf{x}_{t+1} = (1b)$ .

This assumption reflects that the system is initially stable and satisfies all constraints under a nominal controller (e.g., regulated to a stable point using a simple linear feedback law).

In this work, we make no assumptions on boundedness or smoothness properties of  $\mathbf{g}$  (e.g., known Lipschitz constants). Instead, we assume that we have access to a dataset of trajectories generated from sampled parameters  $\xi_j$ . Such information may come from previous operation of a robot in similar environments or data generated from parameterized simulations. This motivates our use of meta-learning to encode this information and characterize the dynamics uncertainty.

#### IV. META-LEARNING & ADAPTATION GUARANTEES

##### A. Bayesian meta-learning

Our approach leverages a model for the unknown dynamics  $\mathbf{g}$ . To this end, we employ the Bayesian meta-learning architecture presented in [18], [45] referred to as ALPACA. Meta-learning (or “learning-to-learn”) [13]–[15] aims to train a model capable of rapid adaptation<sup>1</sup> to a distribution of *tasks*. In this problem setting, a task corresponds to a dynamical system  $\mathbf{g}(\cdot, \cdot, \xi)$  parameterized by the unknown parameters  $\xi$ . ALPACA models the unknown dynamics as

$$\hat{\mathbf{g}}_i(\mathbf{x}, \mathbf{u}) = \theta_i^\top \phi_i(\mathbf{x}, \mathbf{u}), \quad i = 1, \dots, n, \quad (2)$$

where each  $\phi_i : \mathbb{R}^n \times \mathbb{R}^m \rightarrow \mathbb{R}^d$  is a feed-forward neural network and  $\theta_i \in \mathbb{R}^d$  corresponds to the weights of the last layer. The uncertainty in the space of dynamics functions is encoded through a normal distribution on each last layer:  $\theta_i \sim \mathcal{N}(\bar{\theta}_i, \sigma_i^2 \Lambda_i^{-1})$ . As such, each component  $\hat{\mathbf{g}}_i = \langle \theta_i, \phi_i \rangle$  defines

a Gaussian process (GP) with mean function  $\langle \bar{\theta}_i, \phi_i(\mathbf{x}, \mathbf{u}) \rangle$  and kernel  $\sigma_i^2 \phi_i(\mathbf{x}, \mathbf{u})^\top \Lambda_i^{-1} \phi_i(\mathbf{x}', \mathbf{u}')$ .

The basis functions  $\phi_i$  could be chosen as independently-parameterized neural networks. Instead, in this work, we use fully-connected  $L$ -layer neural network basis functions  $\phi_i(\mathbf{z}) = \mathbf{W}_{L+1}^i \tanh(\mathbf{W}_L \tanh \circ \dots \circ \tanh(\mathbf{W}_1 \mathbf{z}))$ , where biases are omitted for conciseness. Sharing the first  $L$  weight matrices across all  $n$  state dimensions allows for efficient scalability of the model and faster offline meta-training compared to training  $n$  separate neural networks  $\phi_i$ . Choosing the bounded tanh activation functions yields smoother mean and variance predictions than common alternatives such as ReLU activations [45], [47]. Finally, the last matrices  $\mathbf{W}_{L+1}^i$  provide an additional degree of freedom which enables each  $i$ -th dimension of the model to select relevant features.<sup>2</sup> We found that using independent neural networks or sharing less than  $L$  weight matrices did not lead to better performance, although our analysis applies to such models as well.

The linear structure of this model allows for efficient online updates whose behavior is well understood. Given a set of transitions from the system  $\{(\mathbf{x}_0, \mathbf{u}_0, \mathbf{x}_1), \dots, (\mathbf{x}_t, \mathbf{u}_t, \mathbf{x}_{t+1})\}$ , we update the last-layer parameters using linear regression via

$$\begin{aligned} \Lambda_{i,t} &= \Phi_{i,t-1}^\top \Phi_{i,t-1} + \Lambda_{i,0}, \\ \bar{\theta}_{i,t} &= \Lambda_{i,t}^{-1} (\Phi_{i,t-1}^\top \mathbf{G}_{i,t} + \Lambda_{i,0} \bar{\theta}_{i,0}), \end{aligned} \quad i = 1, \dots, n, \quad (3)$$

where  $\mathbf{G}_{i,t}^\top = [\mathbf{x}_{i,1} - h_i(\mathbf{x}_0, \mathbf{u}_0), \dots, \mathbf{x}_{i,t} - h_i(\mathbf{x}_{t-1}, \mathbf{u}_{t-1})] \in \mathbb{R}^t$  and  $\Phi_{i,t-1}^\top = [\phi_i(\mathbf{x}_0, \mathbf{u}_0), \dots, \phi_i(\mathbf{x}_{t-1}, \mathbf{u}_{t-1})] \in \mathbb{R}^{d \times t}$ .

**Offline**, this model is meta-trained on a dataset of trajectories corresponding to different system dynamics sampled from the distribution over possible systems. By backpropagating through the posterior predictive distribution to learn the features  $\phi_i$  and the prior parameters  $(\bar{\theta}_{i,0}, \Lambda_{i,0})$ , this model translates a dataset of uncertain trajectories into a learned feature space and a calibrated uncertainty characterization.

<sup>2</sup>The matrices  $\mathbf{W}_{L+1}^i$  also stabilize the offline meta-training process: by weighting intermediate features differently (e.g., when predicting quantities of different units, such as a position versus an angular velocity), this dimension-wise rescaling is not reflected in the precision matrices  $\Lambda_i$  which are then better conditioned. By yielding a larger model class, this additional degree of freedom also allows further regularization to meta-train tighter uncertainty representations, see Section IV-C.

<sup>1</sup>The exact mechanism of “adaptation” to a task is at the core of the meta-learning algorithm. In MAML [15] it consists of a gradient step, in recurrent models it occurs via the hidden state dynamics [46], and in ALPACA [18] the update consists of Bayesian linear regression on the last layer.



More precisely, given  $J$  different sampled dynamics and a meta-training horizon  $T$ , we consider as meta-training objective the joint marginal log likelihood across the data

$$\mathcal{L}(\mathcal{D}_T^J; \bar{\theta}, \Lambda, \phi) = \sum_{j=1}^J \sum_{t=0}^{T-1} \log p(\mathbf{x}_{t+1}^j | \mathbf{u}_{0:t}^j, \mathbf{x}_{0:t}^j), \quad (4)$$

where  $\mathcal{D}_T^J = \{(\mathbf{x}_t^j, \mathbf{u}_t^j, \mathbf{x}_{t+1}^j)_{t=0}^{T-1}\}_{j=1}^J$  is the meta-training dataset and each  $j$ -th trajectory corresponds to the  $j$ -th sampled system (parameterized by  $\xi_j$ ). By meta-training with a Gaussian prior  $\theta_i \sim \mathcal{N}(\bar{\theta}_i, \sigma_i^2 \Lambda_i^{-1})$ , the posterior predictive distribution  $p(\mathbf{x}_{t+1} | \mathbf{u}_{0:t}, \mathbf{x}_{0:t})$  factors in the updates in (3) and evaluates to a Gaussian distribution. (4) then takes a closed-form expression that includes a term that penalizes the deviation of the mean predictions of the model from the training data, as well as a variance term that encourages a model that makes tight uncertainty predictions.

**Online**, using transition tuples  $\{(\mathbf{x}_\tau, \mathbf{u}_\tau, \mathbf{x}_{\tau+1})\}_{\tau=0}^{t-1}$  from the true system, we only adapt the last layer parameters  $\theta_i$  using (3). This restriction on the *online* behavior of the model allows deriving strong adaptation guarantees under reasonable assumptions on the quality of the *offline* training process.

### B. Probabilistic adaptation guarantees

Our first contribution is providing probabilistic adaptation guarantees for this model in the form of uniformly calibrated confidence sets which hold under the following assumptions, which are reasonable for common robotic applications.

**Assumption 2** (Capacity of meta-learned dynamics model) (**A2**). For all possible  $\xi$ , there exists  $\theta_i^*(\xi) \in \mathbb{R}^d$  such that  $\langle \theta_i^*(\xi), \phi_i(\mathbf{x}, \mathbf{u}) \rangle = g_i(\mathbf{x}, \mathbf{u}, \xi) \forall \mathbf{x} \in \mathcal{X}, \forall \mathbf{u} \in \mathcal{U}, i = 1, \dots, n$ .

**Assumption 3** (Calibration of meta-learned prior) (**A3**).

For  $\xi \sim p(\xi)$ , all  $i = 1, \dots, n$ , and  $\delta_i = \delta/(2n)$ ,

$$\mathbb{P}(\|\theta_i^*(\xi) - \bar{\theta}_{i,0}\|_{\Lambda_{i,0}}^2 \leq \sigma_i^2 \chi_d^2(1 - \delta_i)) \geq (1 - \delta_i).$$

These two key assumptions on the quality of the *offline* meta-learning process state that the meta-learning model is capable of fitting the true dynamics (**A2**) and that the prior uncertainty characterization is conservative (**A3**).

In practice, if the dataset has adequate coverage of the state and action spaces and the dynamics distribution  $p(\xi)$ , the offline meta-learning procedure proposed in [18] can approach satisfaction of **A2** and **A3**. Importantly, these assumptions can be empirically verified through predictive performance on a validation dataset, and techniques such as temperature scaling can be used to ensure calibration in a post-hoc manner [48]. **A2** can be relaxed to hold approximately for some approximation error  $\epsilon > 0$ : similar to [20], the resulting analysis would yield larger confidence sets and will be thoroughly investigated in future work. We note that **A3** is weaker than assuming the model is calibrated, a topic extensively studied in the literature [48]. In addition to enabling a theoretical analysis, we also use **A2** and **A3** to derive two regularizers improving the performance and adaptation capabilities of ALPACA; we refer to Section IV-C.

These assumptions, together with the linear structure (2) and adaptation rule (3) of the meta-learned model, allow us

to define adaptive confidence sets over the model parameters  $\theta_i$  that are guaranteed to contain the true parameters  $\theta_i^*$  with high probability, even as the model adapts using process-noise-corrupted measurements.

**Theorem 1** (Uniformly Calibrated Confidence Sets). *Consider the true system (1b), modeled using the meta-learning model (2), which is sequentially updated with online data from (1b) using (3), leading to the updated parameters  $(\bar{\theta}_{i,t}, \Lambda_{i,t})$  for each dimension  $i=1, \dots, n$ . Let*

$$\beta_{i,t}^\delta = \sigma_i \left( \sqrt{2 \log \left( \frac{1}{\delta_i} \frac{\det(\Lambda_{i,t})^{1/2}}{\det(\Lambda_{i,0})^{1/2}} \right)} + \sqrt{\frac{\bar{\lambda}(\Lambda_{i,0})}{\bar{\lambda}(\Lambda_{i,t})} \chi_d^2(1 - \delta_i)} \right) \quad (5)$$

$$\text{and } \mathcal{C}_{i,t}^\delta(\bar{\theta}_{i,t}, \Lambda_{i,t}) = \{\theta_i \mid \|\theta_i - \bar{\theta}_{i,t}\|_{\Lambda_{i,t}} \leq \beta_{i,t}^\delta\}. \quad (6)$$

Then, under Assumptions 2 and 3, for  $\delta_i = \delta/(2n)$ ,

$$\mathbb{P}(\theta_i^* \in \mathcal{C}_{i,t}^\delta(\bar{\theta}_{i,t}, \Lambda_{i,t}) \quad \forall t \geq 0) \geq (1 - 2\delta_i). \quad (7)$$

A proof of this result is available in the Appendix. Using Boole's inequality and Assumptions 2 and 3, it is derived by adapting results from the literature on linear contextual bandits [23], which applies a stopping time argument to bound the probability of the *bad* event that the true parameters lie outside  $\mathcal{C}_{i,t}^\delta$  at some time  $t$ .

Theorem 1 provides confidence sets over model parameters which hold *uniformly over all future times*. This is critical to ensure satisfying the joint chance constraint (1c) despite an unknown final time  $N$ . To do so, we assume there exist fixed true parameters  $\theta_i^*$  corresponding to the true dynamics (**A2**), and we take a frequentist viewpoint such that the confidence set  $\mathcal{C}_{i,t}^\delta$  is a stochastic function of the transition tuples observed online. By defining  $\mathcal{C}_{i,t}^\delta$  through time-dependent values of  $\beta_{i,t}^\delta$ , we ensure that the event that  $\mathcal{C}_{i,t}^\delta$  excludes the true parameters  $\theta_i^*$  at any time  $t$  occurs with probability less than  $(\delta/n)$ .

This scaling factor  $\beta_{i,t}^\delta$  is closely related to that used for Gaussian processes with squared-exponential kernels, for which the value of  $\beta$  is often too large for practical use and is set to a lower value for experiments [21], [22]. In contrast, our model operates within a finite-dimensional feature space and has values of  $\beta$  that are practically usable.

### C. Practical implications for better meta-training

These theoretical results offer guidance on how to add regularization to the offline meta-learning process for the purposes of safe learning-based control. Specifically, we propose to add two regularizers to the offline meta-training of ALPACA. This regularization does not compromise on safety as long as the regularized model still meets assumptions **A2** and **A3**.

**Orthogonal features are better:** Our theory relies on **A2**, which holds as long as each  $g_i$  of the true dynamics lies in the Hilbert space

$$\mathcal{H}_{\phi_i} = \{g: \mathbb{R}^{n+m} \rightarrow \mathbb{R} \mid g = \langle \theta, \phi_i \rangle, \theta \in \mathbb{R}^d\}.$$

Equivalently, **A2** states that each  $g_i$  belongs to the reproducing kernel Hilbert space (RKHS) with kernel  $\sigma_i^2 \phi_i(\cdot, \cdot)^\top \Lambda_i^{-1} \phi_i(\cdot, \cdot)$ . Together, **A2** and **A3** state that with

probability at least  $(1 - \delta_i)$ , each  $g_i$  belongs to the *bounded* RKHS

$$\mathcal{H}_{\phi_i} = \{g: \mathbb{R}^{n+m} \rightarrow \mathbb{R} \mid g = \langle \theta_i, \phi_i \rangle, \|\theta_i - \bar{\theta}_{i,0}\|_{\Lambda_{i,0}}^2 \leq \sigma_i^2 \chi_d^2 (1 - \delta_i)\}.$$

**A2** and **A3** are thus comparable to statements in related work on learning-based control with squared-exponential kernel Gaussian processes. For instance, [21], [22] assume the true dynamics lie in a RKHS of known bounded norm.

This observation suggests that we should meta-learn basis functions  $\phi_i$  corresponding to a *large* space of models  $\mathcal{H}_{\phi_i}$ . Since  $\mathcal{H}_{\phi_i}$  contains linear combinations of the elements of  $\phi_i$ , **A2** thus motivates learning features that are *orthogonal*. To this end, we propose augmenting the meta-learning objective with the following regularizer:

$$\mathcal{L}_{\perp \text{reg}}(\mathbf{W}) = \alpha_{\perp \text{reg}} \sum_{i=1}^n \sum_{\ell=1}^{L+1} \|\mathbf{I}_\ell - \mathbf{W}_\ell^{i\top} \mathbf{W}_\ell^i\|_F^2,$$

where  $\alpha_{\perp \text{reg}} > 0$  controls the strength of this regularization, the  $\mathbf{W}_\ell^i$  are the weights of the neural network basis functions  $\phi_i$ , and each  $\mathbf{I}_\ell$  is an identity matrix of appropriate dimensions. As derived, theoretically analyzed, and empirically validated in [49], this regularizer improves generalization. Also, this term incurs marginal computational overhead compared to the orthogonality regularizer for ALPACA previously proposed in [50] to encourage interpretability of the model. Beyond generalization, for our model with last layer adaptation, orthogonal features also lead to better statistical properties when adapting each  $\theta_i$  through least-squares estimation with (3), see [51].

**$\beta$ -regularization:** Another aspect which can be regularized during offline meta-learning to improve downstream performance is  $\beta_i$ , which controls the size of the confidence sets for the model parameters  $\theta_i$ . With expressive neural network features  $\phi_i$ , multiple settings of the neural network weights and of the prior parameters  $(\bar{\theta}_{i,0}, \Lambda_{i,0})$  can yield a model satisfying assumptions 2 and 3. In this case, it is preferable to select features and prior parameters that lead to lower values of  $\beta_i$ . To do so, we propose adding regularization to encourage meta-learning representations with lower values of  $\beta_i$  without compromising on safety.

We note from (5) that the value of each  $\beta_i$  depends on the ratio between the maximum and minimum eigenvalues of the prior and posterior precision matrices  $\Lambda_i$ . If  $\bar{\lambda}(\Lambda_{i,0}) \leq 1$  (which can be enforced by rescaling the features  $\phi_i$ ), then

$$\frac{\bar{\lambda}(\Lambda_{i,0})}{\bar{\lambda}(\Lambda_{i,t})} = \frac{\bar{\lambda}(\Lambda_{i,t}^{-1})}{\bar{\lambda}(\Lambda_{i,0}^{-1})} \leq \bar{\lambda}(\Lambda_{i,t}^{-1}) \bar{\lambda}(\Lambda_{i,0}^{-1}) \leq \bar{\lambda}(\Lambda_{i,t}^{-1}) \bar{\lambda}(\Lambda_{i,0}^{-1}).$$

Furthermore,  $\bar{\lambda}(\Lambda) \leq \sqrt{\text{Tr}(\Lambda^T \Lambda)}$ . Combining with the above, we propose to regularize an upper bound of the ratios  $\bar{\lambda}(\Lambda_{i,0})/\bar{\lambda}(\Lambda_{i,t})$  during offline meta-training:

$$\mathcal{L}_{\text{reg}}(\Lambda_0) = \alpha_{\text{reg}} \sum_{i=1}^n \text{Tr}(\Lambda_{i,t}^{-T} \Lambda_{i,t}^{-1}) \text{Tr}(\Lambda_{i,0}^{-T} \Lambda_{i,0}^{-1}) \quad (8)$$

where  $\alpha_{\text{reg}} > 0$  controls the strength of this regularization and is selected using a validation dataset and  $T$  is the meta-training horizon. As the model is directly parameterized by the inverse

of the precision matrices  $\Lambda_i$  [45], this regularizer can easily be added to the standard training loss (4).

From (5), we observe that  $\beta_i$  also depends on the ratio of determinants of the prior and posterior precision matrices  $\det(\Lambda_{i,t})/\det(\Lambda_{i,0})$ . Although a convex regularizer for this term can be derived, we found that including it did not lead to performance improvements. This ratio can be interpreted as capturing the amount of information that the model has gathered online, which is independent of the structure of the prior model. Before learning, this ratio is 1, so the other term composed of the ratio of eigenvalues dominates  $\beta_i$ . We observed that it is during these early stages that the meta-training model and its bounds  $\beta_i$  are most conservative, which could explain the importance of the regularizer in (8), whereas regularizing the ratio of determinants appears to make little difference.

## V. SEQUENTIAL EXPLORATION AND EXPLOITATION FOR LEARNING SAFELY (SEELS)

In order to ensure safety at all times with high probability and eventually reach  $\mathcal{X}_{\text{goal}}$ , we provide a conservative deterministic reformulation of CC-OCP, propose an algorithm tackling problems with high uncertainty, analyze its safety and feasibility properties, and discuss implementation.

### A. Relaxation of CC-OCP using reachability analysis

In order to reason about how parameter uncertainty manifests in terms of potential system behavior in the state space (and whether it might violate safety constraints), we translate confidence sets over parameters into confidence *tubes* over trajectories. We stress that confidence tubes jointly depending on the parameters are required to satisfy the joint chance constraint (1c), since enforcing a single chance constraint at each timestep as in [24], [27]–[30] does not guarantee safety of the whole trajectory [31], [32].

We construct these tubes by leveraging the confidence sets  $\mathcal{C}_{i,t}^\delta$ . Indeed, a direct consequence of Theorem 1 is that

$$\mathbb{P}(\exists \theta_i \in \mathcal{C}_{i,t}^\delta(\bar{\theta}_{i,t}, \Lambda_{i,t}) \forall t \geq 0 \text{ s.t. } \langle \theta_i, \phi_i \rangle = g_i) \geq (1 - 2\delta_i).$$

This implies that a control trajectory respecting all constraints for all  $\theta_i \in \mathcal{C}_{i,t}^\delta$  and  $\epsilon^i \in \mathcal{E}_i$  also satisfies (1c). Thus, to conservatively reformulate (1c), we propose performing reachability analysis using the sets  $\mathcal{C}_{i,t}^\delta$  and  $\mathcal{E}_i$ . Specifically, given a sequence of open-loop control inputs  $\mathbf{u} = (\mathbf{u}_0, \dots, \mathbf{u}_{N-1})$ , we define the sequence of reachable sets<sup>3</sup>

$$\mathcal{X}_k^{t,\delta}(\mathbf{u}) = \left\{ \mathbf{x}_k = \mathbf{f}(\cdot, \mathbf{u}_{k-1}, \boldsymbol{\theta}, \boldsymbol{\epsilon}_{k-1}) \circ \dots \circ \mathbf{f}(\mathbf{x}_0, \mathbf{u}_0, \boldsymbol{\theta}, \boldsymbol{\epsilon}_0) \mid \mathbf{x}_0 = \mathbf{x}(t), \boldsymbol{\theta}_i \in \mathcal{C}_{i,t}^\delta, \boldsymbol{\epsilon}_s^i \in \mathcal{E}_i, s=1, \dots, k-1, i=1, \dots, n \right\}, \quad (9)$$

where  $k=1, \dots, N$  and  $f_i(\mathbf{x}, \mathbf{u}, \boldsymbol{\theta}, \boldsymbol{\epsilon}) = h_i(\mathbf{x}, \mathbf{u}) + \boldsymbol{\theta}_i^\top \boldsymbol{\phi}_i(\mathbf{x}, \mathbf{u}) + \epsilon^i$ .

<sup>3</sup>This definition closely follows [52] for the specific case of a sequence of open-loop control inputs. One can account for a nominal feedback controller as a simple extension to reduce the tube size [22], [24], [27], [52]. In our simulated experiments, we omit feedback to better demonstrate the adaptation capabilities of the meta-training model, show the tightness of the confidence sets, and better verify the safety claims of the framework.

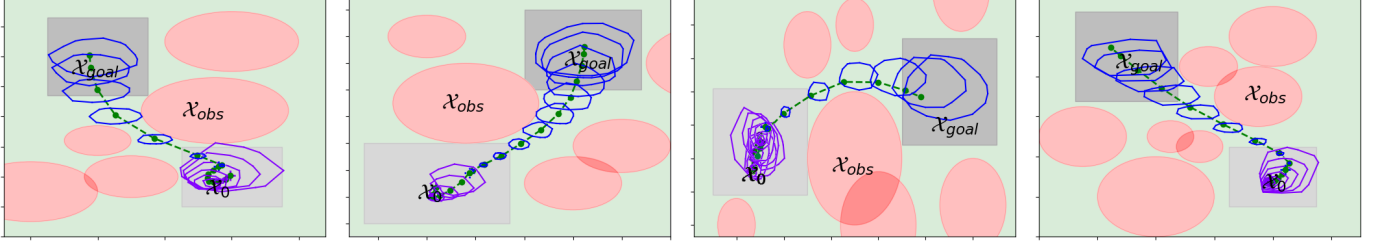


Fig. 3. Initially, uncertainty is too high to safely reach the goal. Instead, we plan safe information-gathering trajectories to infer the dynamics and reduce uncertainty. Once planning to  $\mathcal{X}_{\text{goal}}$  is feasible, the robot can safely reach the goal while satisfying all constraints with high probability. Color legend: **true trajectory**, **reachable sets for exploration** (9), **reachable sets for exploitation**. This experiment is described in Section VI-B.

Quantifying uncertainty regarding the system dynamics and the online learning process as confidence sets on the model parameters  $\theta$  and subsequently transforming these sets into reachable sets in the state space enables the relaxation of the original chance-constrained problem into a deterministic one:

#### REACH-OCF

$$\min_{\mu, u} \sum_{k=0}^N \ell(\mu_k, u_k) \text{ s.t. } \bigwedge_{k=1}^N \mathcal{X}_k^{t, \delta} \subset \mathcal{X}_{\text{free}}, \mathcal{X}_N^{t, \delta} \subset \mathcal{X}_{\text{goal}}, \\ \bigwedge_{k=0}^{N-1} u_k \in \mathcal{U}, \mathcal{X}_0^{t, \delta} = \{x(t)\},$$

where  $\mu = (\mu_0, \dots, \mu_N)$  are the centers of the reachable sets  $\{\mathcal{X}_k^{t, \delta}\}_{k=1}^N$ , which depend on  $(\mu, u)$  and satisfy (9). We use a mean-equivalent reformulation of the expected cost<sup>4</sup>, as this work is mostly concerned with reaching  $\mathcal{X}_{\text{goal}}$  while satisfying constraints at all times. Further, the cost typically penalizes open-loop control inputs, which are deterministic.

#### B. SEELS: algorithm for safe learning and reaching $\mathcal{X}_{\text{goal}}$

Due to high dynamics uncertainty, tight control constraints, and long planning horizons, REACH-OCF may be infeasible. This motivates a safe learning-based exploration-exploitation framework to sequentially reduce uncertainty and eventually reach  $\mathcal{X}_{\text{goal}}$ . Our approach is based on a repeated two-phase approach: when REACH-OCF is feasible, we enter the *exploitation* phase and plan a safe trajectory to  $\mathcal{X}_{\text{goal}}$  with the current model uncertainty. In the *exploration* phase, we instead strictly perform safe exploration, planning an information-gathering trajectory that returns to the initial safe invariant set  $\mathcal{X}_0$ . The corresponding robust optimal control problem is written as

#### EXPLORE-OCF

$$\max_{\mu, u} \sum_{k=0}^N (\ell + \ell_{\text{info}})(\mu_k, u_k) \text{ s.t. } \bigwedge_{k=1}^N \mathcal{X}_k^{t, \delta} \subset \mathcal{X}_{\text{free}}, \mathcal{X}_N^{t, \delta} \subset \mathcal{X}_0, \\ \bigwedge_{k=0}^{N-1} u_k \in \mathcal{U}, \mathcal{X}_0^{t, \delta} = \{x(t)\},$$

where the sequence of reachable sets  $\{\mathcal{X}_k^{t, \delta}\}_{k=1}^N$  satisfies (9). EXPLORE-OCF is similar to REACH-OCF but instead uses  $\mathcal{X}_0$  as the final set, thus ensuring the system is safe for the next

<sup>4</sup>As we use a sampling-based approach to compute the reachable sets [52], the variance associated with these samples could be used to approximate the variance of the cost, or minimize a given risk metric [53].

---

#### Algorithm 1 Sequential Exploration and Exploitation for Learning Safely (SEELS)

---

**Input:** Meta-training model satisfying A.2 and A.3

```

1: while  $x_0 \notin \mathcal{X}_{\text{goal}}$  do
2:   for  $N_i \in \{N_{\text{reach}}, \dots, \bar{N}_{\text{reach}}\}$  do  $\triangleright$  Try reaching
3:      $(\mu, u) \leftarrow$  Solve REACH-OCF
4:     if REACH-OCF feasible then
5:       Apply  $u_{0:N-1}$  to true system  $\triangleright$  Reach
6:       Break
7:   for  $N_i \in \{1, \dots, N_{\text{info}}\}$  do  $\triangleright$  Explore
8:      $(\mu^i, u^i) \leftarrow$  Solve EXPLORE-OCF
9:     if EXPLORE-OCF feasible then
10:      Compute  $\ell_{\text{info}}^i(\mu^i, u^i)$ 
11:    $i_{\text{best}} \leftarrow \arg \max_i \ell_{\text{info}}^i(\mu^i, u^i)$   $\triangleright$  Get best  $N$ 
12:   Apply  $u^{i_{\text{best}}}$  to true system
13:   Update  $(\theta, \Lambda)$  with  $\{(x_k, u_k, x_{k+1})\}_{k=0}^{N-1}$   $\triangleright$  Learn
14:    $x_0 \leftarrow x_N$ 

```

---

phase with high probability, and it further uses an information-gathering cost function  $\ell_{\text{info}}$  to encourage visiting states which reduce remaining uncertainty in the dynamics

$$\ell_{\text{info}}(x, u) = \frac{1}{2} \sum_{i=1}^n \log(1 + \phi_i(x, u)^\top \Lambda_{i,t}^{-1} \phi_i(x, u)), \quad (10)$$

which we derive from the mutual information between the unknown dynamics and the observations in the next section.

**SEELS:** We summarize our approach in Algorithm 1 (SEELS), which consists of iteratively learning a model of the dynamics by solving EXPLORE-OCF before reaching  $\mathcal{X}_{\text{goal}}$  when REACH-OCF admits a feasible solution. This split yields a tractable sequence of trajectory optimization problems, although it induces sub-optimality relative to the computationally intractable problem of simultaneous exploration and exploitation [54]. Since *safely* learning nonlinear dynamics with minimal assumptions remains an open area of research (see Section II), quantifying this sub-optimality gap (perhaps by computing the regret of the algorithm) is beyond the scope of this work.

### C. Information objective

During the exploration phase, we perform trajectory optimization with an objective function  $\ell_{\text{info}}$  that encourages visiting states and taking actions that reduce uncertainty over the unknown dynamics. To do so, a natural objective to maximize is the mutual information between the unknown dynamics  $\mathbf{g}$  and the observations of the state. This cost characterizes the *information gain* [55]–[57] about  $\mathbf{g}$ , gained from applying the control inputs  $\mathbf{u}$  to the true system from a state  $\mathbf{x}$ , and observing the next state corrupted by random disturbances.

To derive this objective, we leverage the Bayesian interpretation of ALPACA which is used during offline meta-training to obtain a model that has the correct structure (Assumption 2) and is calibrated (Assumption 3). Specifically, ALPACA is trained assuming zero-mean Gaussian-distributed observation noise  $\epsilon_t^i$  of variance  $\sigma_i^2$  and a Gaussian prior over model parameters  $\theta_i \sim \mathcal{N}(\bar{\theta}_{i,0}, \sigma_i^2 \Lambda_{i,0}^{-1})$ . Using (3) and  $t$  transitions from the system, this yields the posterior distribution  $\theta_i \sim \mathcal{N}(\bar{\theta}_i, \sigma_i^2 \Lambda_{i,t}^{-1})$ . In this setting, the marginal distribution over observations  $\tilde{x}_{t+1}^+ = x_{t+1,i} - h_i(x_t, \mathbf{u}_t) = \theta_i \phi_i(x_t, \mathbf{u}_t) + \epsilon_t^i$  given an arbitrary state  $\mathbf{x}_t$  and control input  $\mathbf{u}_t$  is a normal distribution  $\mathcal{N}(\bar{\theta}_i \phi_i, (1 + \phi_i^T \Lambda_{i,t}^{-1} \phi_i) \sigma_i^2)$ , where  $\phi_i = \phi_i(x_t, \mathbf{u}_t)$ .

For this formulation, the mutual information  $\mathcal{I}$  between the observation  $\tilde{x}^+ = x_{t+1} - \mathbf{h}(x_t, \mathbf{u}_t)$  and the true unknown dynamics  $\mathbf{g}$  can be derived in closed-form. It is defined using the entropy  $\mathcal{H}(\cdot)$ , which for a random variable  $\mathbf{x}^+ \sim \mathcal{N}(\boldsymbol{\mu}, \boldsymbol{\Sigma})$  evaluates to  $\mathcal{H}(\mathbf{x}) = (1/2) \log(\det(2\pi e \boldsymbol{\Sigma}))$ . Hence, the information gain from observing the scalar random variable  $x_i^+$  can be expressed as  $\mathcal{I}(x_i^+; g_i) = \mathcal{H}(x_i^+) - \mathcal{H}(x_i^+ | g_i) = \frac{1}{2} (\log(\text{var}(x_i^+)) - \log(\text{var}(x_i^+ | g_i))) = \frac{1}{2} (\log((1 + \phi_i^T \Lambda_{i,t}^{-1} \phi_i) \sigma_i^2) - \log(\sigma_i^2)) = \frac{1}{2} (\log(1 + \phi_i^T \Lambda_{i,t}^{-1} \phi_i))$ . This quantity expresses the information gain from observing each dimension  $i$  of the state, which are modeled independently in our formulation. By summing  $\mathcal{I}(x_i^+; g_i)$  over  $i = 1, \dots, n$ , we arrive at the exploration objective  $\ell_{\text{info}}$  in (10).

The objective  $\ell_{\text{info}}$  is a function of the current information state of the model, specified by the updated precision matrices  $\Lambda_{1,t}, \dots, \Lambda_{n,t}$ . It explicitly encourages taking actions and visiting states in the feature space spanned by  $\phi$  which have highest variance  $\Lambda_{1,t}^{-1}$ . The resulting observations are then the most informative in terms of reducing uncertainty over  $\mathbf{g}$ .

Note that the expected information gain along a trajectory is not simply the sum of the expected information gains per transition, as expressed in EXPLORE-OCP when summing (10) over  $k=0, \dots, N$ . However, correctly computing the expected information gain along the trajectory would require factoring in model updates along the trajectory; we find that considering the sum of single-transition information gain with the current precision matrices  $\Lambda_{i,t}$  is sufficient in guiding exploration. Also, while in this work we assume bounded (non-Gaussian) noise corrupting our measurements and derive (frequentist) confidence sets for the parameters of the last layer of the model, we find that making this approximation works well in practice to encourage exploration. The problem of optimal exploration is beyond the scope of this framework.

Finally, we note that this cost function  $\ell_{\text{info}}$  does not suffer

from computational complexity scaling with the amount of data, as is the case for similar objectives derived for squared-exponential kernel GPs [22], [56]. This computational efficiency comes from choosing finite-dimensional basis functions to parameterize the model class for the true dynamics  $\mathbf{g}$ .

### D. Probabilistic safety and feasibility guarantees

This approach enjoys probabilistically guaranteed safety and ensures that EXPLORE-OCP remains feasible at all times with high probability, which is crucial to enable autonomous operation. Our next result also states that provided that REACH-OCP is eventually feasible, then the agent will safely reach  $\mathcal{X}_{\text{goal}}$  with high probability. This result characterizes our proposed approach as a feasible solution to CC-OCP.

**Theorem 2** (Probabilistic recursive feasibility and safety). *Using the confidence sets defined in (6) and the reachable sets satisfying (9), apply SEELS and sequentially solve EXPLORE-OCP and REACH-OCP. Then,*

- *There exists optimization horizons  $N_j$  ensuring the feasibility of each  $j$ -th exploration problem EXPLORE-OCP $_j$  with probability at least  $(1 - \delta)$ .*
- *Assuming that REACH-OCP is eventually feasible, the system is guaranteed to satisfy (1c), i.e., to be safe at all times and eventually reach  $\mathcal{X}_{\text{goal}}$  with probability at least  $(1 - \delta)$ .*

*Proof.* First, we prove that SEELS is recursively feasible with high probability, before proving that the system satisfies (1c).

*Probabilistic recursive feasibility:* Let  $n_{\text{info}}$  be the number of exploration phases before REACH-OCP becomes feasible<sup>5</sup>. Also, let  $N_{\text{info}}^j$ , and  $t_j = \sum_{l=0}^{j-1} N_{\text{info}}^l$  be, respectively, the planning horizon, and the start time index of each EXPLORE-OCP $_j$ . For conciseness, define **(EOCP)** $_j$  for  $\{\text{EXPLORE-OCP}_j \text{ is feasible}\}$ , corresponding to the event that the  $j$ -th exploration problem is feasible. Then,

$$\begin{aligned} \mathbb{P}\left(\bigwedge_{j=0}^{n_{\text{info}}} (\text{EOCP})_j\right) &\geq \mathbb{P}\left(\bigwedge_{j=0}^{n_{\text{info}}} (\text{EOCP})_j, \mathbf{x}_{t_{n_{\text{info}}}} \in \mathcal{X}_0\right) \\ &= \mathbb{P}\left((\text{EOCP})_{n_{\text{info}}} \mid \bigwedge_{j=0}^{n_{\text{info}}-1} (\text{EOCP})_j, \mathbf{x}_{t_{n_{\text{info}}}} \in \mathcal{X}_0\right) \\ &\quad \cdot \mathbb{P}\left(\bigwedge_{j=0}^{n_{\text{info}}-1} (\text{EOCP})_j, \mathbf{x}_{t_{n_{\text{info}}}} \in \mathcal{X}_0\right). \end{aligned}$$

By Assumption 1, given that  $\mathbf{x}_{t_j} \in \mathcal{X}_0$ , EXPLORE-OCP $_j$  is feasible for any  $j$ -th exploration phase. Indeed, choose  $N_{\text{info}}^j = 1$  for EXPLORE-OCP $_j$ . Then,  $\mathbf{u}_0^j = \pi(\mathbf{x}_{t_j})$  is a feasible solution to EXPLORE-OCP $_j$ . Thus, the event  $\{(\text{EOCP})_j \mid \mathbf{x}_{t_j} \in \mathcal{X}_0\}$  holds with probability one. In particular, this implies that the event

$$\{(\text{EOCP})_{n_{\text{info}}} \mid \bigwedge_{j=0}^{n_{\text{info}}-1} (\text{EOCP})_j, \mathbf{x}_{t_{n_{\text{info}}}} \in \mathcal{X}_0\}$$

holds with probability one.

<sup>5</sup>This result also holds if CC-OCP is not feasible, and the algorithm can never solve REACH-OCP (e.g., if  $\mathcal{X}_{\text{goal}}$  is surrounded by obstacles). Indeed, if the algorithm is stuck in an infinite number of exploration steps, the last inequality of this proof still holds for  $n_{\text{info}} \rightarrow \infty$ , by Theorem 1.



Next, we leverage our confidence sets:

$$\begin{aligned}
\mathbb{P}\left(\bigwedge_{j=0}^{n_{\text{info}}}(\mathbf{EOCP})_j\right) &\geq \mathbb{P}\left(\bigwedge_{j=0}^{n_{\text{info}}-1}(\mathbf{EOCP})_j, \mathbf{x}_{t_{n_{\text{info}}}} \in \mathcal{X}_0\right) \\
&\geq \mathbb{P}\left(\bigwedge_{j=0}^{n_{\text{info}}-1}(\mathbf{EOCP})_j, \mathbf{x}_{t_{n_{\text{info}}}} \in \mathcal{X}_0, \boldsymbol{\theta}_i^* \in \mathcal{C}_{i,t_{n_{\text{info}}}-1}^\delta \forall i\right) \\
&= \mathbb{P}\left(\mathbf{x}_{t_{n_{\text{info}}}} \in \mathcal{X}_0 \mid \bigwedge_j(\mathbf{EOCP})_j, \boldsymbol{\theta}_i^* \in \mathcal{C}_{i,t_{n_{\text{info}}}-1}^\delta \forall i\right) \\
&\quad \cdot \mathbb{P}\left(\bigwedge_j(\mathbf{EOCP})_j, \boldsymbol{\theta}_i^* \in \mathcal{C}_{i,t_{n_{\text{info}}}-1}^\delta \forall i\right).
\end{aligned}$$

By construction of the reachable sets  $\{\mathcal{X}_k^{t_j,\delta}\}_{k=1}^{N_{\text{info}}^j}$ , by Assumption 2, and by definition of EXPLORE-OC<sub>j</sub> (since  $\mathcal{X}_{N_{\text{info}}^j}^{t_j,\delta} \subset \mathcal{X}_0$ ), we have that  $\mathbf{x}_{t_{j+1}} \in \mathcal{X}_0$  given that EXPLORE-OC<sub>j</sub> is feasible and  $\boldsymbol{\theta}_i^* \in \mathcal{C}_{i,t_j}^\delta \forall i$ , for any  $j$ -th exploration problem.

Thus, the first term  $\{\mathbf{x}_{t_{n_{\text{info}}}} \in \mathcal{X}_0 \mid \bigwedge_j(\mathbf{EOCP})_j, \boldsymbol{\theta}_i^* \in \mathcal{C}_{i,t_{n_{\text{info}}}-1}^\delta \forall i\}$  holds with probability one, and

$$\mathbb{P}\left(\bigwedge_{j=0}^{n_{\text{info}}}(\mathbf{EOCP})_j\right) \geq \mathbb{P}\left(\bigwedge_{j=0}^{n_{\text{info}}-1}(\mathbf{EOCP})_j, \boldsymbol{\theta}_i^* \in \mathcal{C}_{i,t_{n_{\text{info}}}-1}^\delta \forall i\right).$$

Since  $(\mathbf{EOCP})_0$  is feasible with probability one since  $\mathbf{x}_0 \in \mathcal{X}_0$ , and by reasoning by induction for all  $j = n_{\text{info}}, \dots, 0$ , we obtain that

$$\mathbb{P}\left(\bigwedge_{j=0}^{n_{\text{info}}}(\mathbf{EOCP})_j\right) \geq \mathbb{P}\left(\bigwedge_{j=0}^{n_{\text{info}}-1} \boldsymbol{\theta}_i^* \in \mathcal{C}_{i,t_j}^\delta \forall i\right) \geq (1 - \delta),$$

where the last inequality comes from Theorem 1.

*Probabilistic safety:* Let also  $N_{\text{reach}}$ , and  $t_f$  be, respectively, the planning horizon, and the start time index of REACH-OC<sub>P</sub>. For conciseness, define  $\mathbf{x}_k^{t_j} = \mathbf{x}_{t_j+k}$ , corresponding to the state at time  $(t_j+k)$  in the  $j$ -th phase. Note that without feedback, open-loop controls satisfy  $\mathbf{u}_t \in \mathcal{U} \forall t$ . Further, define the event that the trajectory during the  $j$ -th exploration phase (or exploitation phase) satisfies all constraints as

$$\begin{aligned}
\{\mathbf{x}_{\text{info}}^j \in \mathcal{X}_{\text{info}}^j\} &= \left\{ \bigwedge_{k=1}^{N_{\text{info}}^j} (\mathbf{x}_k^{t_j} \in \mathcal{X}_{\text{free}}) \wedge (\mathbf{x}_{N_{\text{info}}^j}^{t_j} \in \mathcal{X}_0) \right\}, \\
\{\mathbf{x}_{\text{reach}} \in \mathcal{X}_{\text{reach}}\} &= \left\{ \bigwedge_{k=1}^{N_{\text{reach}}} (\mathbf{x}_k^{t_f} \in \mathcal{X}_{\text{free}}) \wedge (\mathbf{x}_{N_{\text{reach}}}^{t_f} \in \mathcal{X}_{\text{goal}}) \right\},
\end{aligned}$$

where  $j = 1, \dots, n_{\text{info}}$ . With this notation, we rewrite the probabilistic safety constraint of the original problem as

$$\begin{aligned}
(1c) &= \mathbb{P}\left(\bigwedge_{j=1}^{n_{\text{info}}} \{\mathbf{x}_{\text{info}}^j \in \mathcal{X}_{\text{info}}^j\} \wedge \{\mathbf{x}_{\text{reach}} \in \mathcal{X}_{\text{reach}}\}\right) \triangleq \mathbb{P}(\{\text{Success}\}) \\
&\geq \mathbb{P}(\{\text{Success}\} \mid \boldsymbol{\theta}_i^* \in \mathcal{C}_{i,t}^\delta \forall t \forall i) \mathbb{P}(\boldsymbol{\theta}_i^* \in \mathcal{C}_{i,t}^\delta \forall t \forall i), \quad (11)
\end{aligned}$$

where  $t = t_1, \dots, t_{n_{\text{info}}}, t_f$ , and  $i = 1, \dots, n^6$ . Again, by Assumption 2, the meta-learning model can fit the true dynamics. Hence, if the true parameters are within the confidence sets

<sup>6</sup>The inequality follows from  $(1c) = \mathbb{P}(\{\text{Success}\} \mid \boldsymbol{\theta}_i^* \in \mathcal{C}_{i,t}^\delta \forall t \forall i) \mathbb{P}(\boldsymbol{\theta}_i^* \in \mathcal{C}_{i,t}^\delta \forall t \forall i) + \mathbb{P}(\{\text{Success}\} \mid \boldsymbol{\theta}_i^* \notin \mathcal{C}_{i,t}^\delta \forall t, \forall i) \mathbb{P}(\boldsymbol{\theta}_i^* \notin \mathcal{C}_{i,t}^\delta \forall t, \forall i) \geq (11)$ .

$\mathcal{C}_{i,t}^\delta$ , then, the reachable sets  $\mathcal{X}_k^{t,\delta}$  defined in (9) necessarily contain the state trajectory on the true system. Hence,

$$\{\mathcal{X}_k^{t,\delta} \subset \mathcal{X}_{\text{free}}\} = \{\mathbf{x}_k(\boldsymbol{\theta}^*) \in \mathcal{X}_{\text{free}} \mid \boldsymbol{\theta}_i^* \in \mathcal{C}_{i,t}^\delta, \forall i\}. \quad (12)$$

By definition of EXPLORE-OC<sub>P</sub> and REACH-OC<sub>P</sub>, the reachable sets are subsets of the safe set (with probability one), and

$$\begin{aligned}
\mathbb{P}(\mathbf{x}_k^t(\boldsymbol{\theta}^*) \in \mathcal{X}_{\text{free}}, k=1, \dots, N \mid \boldsymbol{\theta}_i^* \in \mathcal{C}_{i,t}^\delta, i=1, \dots, n) \\
= \mathbb{P}(\mathcal{X}_k^{t,\delta} \subset \mathcal{X}_{\text{free}}, k=1, \dots, N) = 1,
\end{aligned}$$

which also holds for the final constraints  $\mathbf{x}_N^t \in \mathcal{X}_0$ , and  $\mathbf{x}_N^{t_f} \in \mathcal{X}_{\text{goal}}$ . Thus,  $\mathbb{P}(\{\text{Success}\} \mid \boldsymbol{\theta}_i^* \in \mathcal{C}_{i,t}^\delta \forall t \forall i) = 1$ . Combining this result with (11), we obtain that the system satisfies all constraints and eventually reaches  $\mathcal{X}_{\text{goal}}$  with probability at least the probability of the model parameters belonging to the confidence sets, i.e.,  $(1c) \geq \mathbb{P}(\boldsymbol{\theta}_i^* \in \mathcal{C}_{i,t}^\delta \forall t \forall i)$ . This last term holds with probability greater than  $(1-\delta)$ . Indeed, using (a) Boole's inequality, and (b) Theorem 1, we obtain that

$$\begin{aligned}
(1c) &\geq \mathbb{P}(\boldsymbol{\theta}_i^* \in \mathcal{C}_{i,t}^\delta \forall t \forall i) = 1 - \mathbb{P}\left(\bigvee_{i=1}^n \bigvee_t \boldsymbol{\theta}_i^* \notin \mathcal{C}_{i,t}^\delta\right) \\
&\stackrel{(a)}{\geq} 1 - \sum_{i=1}^n \mathbb{P}\left(\bigvee_t \boldsymbol{\theta}_i^* \notin \mathcal{C}_{i,t}^\delta\right) = 1 - \sum_{i=1}^n \left(1 - \mathbb{P}\left(\bigwedge_t \boldsymbol{\theta}_i^* \in \mathcal{C}_{i,t}^\delta\right)\right) \\
&\stackrel{(b)}{\geq} 1 - \sum_{i=1}^n (1 - (1 - 2\delta_i)) = 1 - \sum_{i=1}^n (2\delta_i) = (1 - \delta)
\end{aligned}$$

since  $\delta_i = \delta/(2n)$ . This concludes the proof of Theorem 2.  $\square$

Key to this proof are Theorem 1 and the definition of the reachable sets in (9). We stress that our safety probability  $(1 - \delta)$  is independent of the (unknown) time to reach  $\mathcal{X}_{\text{goal}}$ , which would not be the case if pointwise chance constraints were used instead of (1c).

Theorem 2 relies on REACH-OC<sub>P</sub> eventually becoming feasible. If the original problem is feasible with perfect knowledge of the dynamics, we can ensure this assumption holds by guaranteeing that the objective used for *exploration* leads to actions that continually reduce uncertainty in dynamics using conditions on observability and persistence of excitation [4], [6], [10], which are satisfied in practice with full state information, meta-learned features, and long exploration horizons using our information cost. In situations where the problem is not feasible in the first place (e.g., an obstacle blocks the only path to  $\mathcal{X}_{\text{goal}}$ ), our algorithm defaults to exploring within a feasible neighborhood around  $\mathcal{X}_0$ , in which case the system is guaranteed to satisfy all safety constraints at all times with probability greater than  $(1 - \delta)$ .

By assuming bounded disturbances  $\epsilon$  and exploiting confidence sets over the model parameters which hold jointly for all times with high probability (Theorem 1), we can guarantee the feasibility of EXPLORE-OC<sub>P</sub> during exploration. This contrasts with related work in the MPC literature which provides probabilistic recursive feasibility over a finite horizon only [58]. This aspect is crucial to enable autonomous operation and reliability of the approach.

### E. Implementation and practical considerations

Implementation of the algorithm is complicated by challenges in reachability analysis and non-convex optimization.

**Reachability Analysis:** Computing the reachable sets in (9) is difficult due to the non-convexity of the features  $\phi$ . Methods reasoning about single-step set propagation (e.g., [22]) are generally too conservative [52] as they neglect time correlations induced by the parameters  $\theta_i$ . Moreover, the online updates to the model parameter preclude exact methods which perform computations offline to compute reachable sets, e.g., [59], [60]. Neural network verification techniques [61] are tailored to offline computations and are not yet fast enough for online trajectory optimization. Finally, methods using Lipschitz continuity can provide conservative reachable set approximations [22], but such techniques would be so conservative for the systems we consider in this work that the agent would never deem reaching the goal to be feasible, even if one had access to the true Lipschitz constant of the system. The main limitation of [22] is that it adopts a single-step worst case analysis and does not account for the time correlations of the parameters [52].

For these reasons, we leverage a recently-derived sampling-based uncertainty propagation scheme for reachability analysis (RANDUP) [52]. By sampling parameters  $(\theta_i, \epsilon)$  within their confidence sets, computing reachable states  $\mathbf{x}$  for these parameters, and approximating the reachable sets in (9) by their convex hull, RANDUP provides a scalable approach to compute these tubes with minimal assumptions on the system's dynamics, enabling the use of arbitrary neural network features  $\phi$ . It is fast enough to be used with common robotic systems (computing a trajectory requires less than a second for a 13-dimensional spacecraft system with a Python implementation [52]) and can be further accelerated through parallelization on GPUs. Although this method lacks finite-sample guarantees of safety, asymptotic guarantees can be derived using random set theory, and finite-sample approximations are sufficient to ensure safety in practice, as demonstrated in our results.

**Optimization-based planning:** Using RANDUP, we reframe a generally intractable stochastic optimal control problem into EXPLORE-OCF and REACH-OCF, which are non-convex optimal control problems. Efficiently computing solutions is an active field of research which we address through a direct method based on sequential convex programming (SCP) [27]. By solving a sequence of convexified versions of the original problem, SCP-based methods can run in real time and provide theoretical guarantees of local optimality [62], [63] given an initialization within the correct homotopy class. In this work, we initialize each method with an infeasible straight-line trajectory, solve each convexified problem using OSQP [64] and provide further details in Appendix B.

Additionally, due to uncertainty, the feasibility of each problem depends on the optimization horizon  $N$ . For this reason, Algorithm 1 performs a search over a predefined range of planning horizons (lines 2 and 7). For exploitation, it selects the first feasible solution if one exists, although other criteria could be used, e.g., minimal control cost. For exploration, we select the trajectory which leads to the largest expected

information gain. Indeed, due to tight control constraints and safety constraints, a longer horizon does not necessarily lead to higher information gain. This heuristic works well in practice, and future work will adopt a continuous-time problem formulation with free final time, which is an active area of research [63].

## VI. SIMULATION STUDIES

### A. Robotic manipulation in a cluttered environment

First, consider the three-link open-chain torque-controlled manipulator shown in Figure 4 [65]. The state of the system is  $\mathbf{x} = (q_1, q_2, q_3, \dot{q}_1, \dot{q}_2, \dot{q}_3)$  and its control is  $\mathbf{u} = (\tau_1, \tau_2, \tau_3)$ , where  $q_i$  is the angle of the  $i$ -th joint and  $\tau_i$  is its torque. Its true dynamics follow

$$M(\mathbf{q})\ddot{\mathbf{q}} + C(\mathbf{q}, \dot{\mathbf{q}})\dot{\mathbf{q}} + N(\mathbf{q}) = \mathbf{u}, \quad (13)$$

where  $\mathbf{q} = (q_1, q_2, q_3)$ . The expressions for  $M(\mathbf{q})$ ,  $C(\mathbf{q}, \dot{\mathbf{q}})$ , and  $N(\mathbf{q})$  depend on the lengths  $l_1 = 1$  m,  $l_2 = l_3 = 0.5$  m, masses  $m_i$ , and inertias  $I_i$  of each  $i$ -th link of the manipulator (see [65]). By introducing uncertainty in each  $m_i$  and  $I_i$ , this experiment corresponds to a scenario where the robot must manipulate uncertain payloads and identify its inertial properties. Although manipulators are often controlled using trajectory generation and high-frequency low-level tracking, the instability of this system makes it a useful case study for our framework.

Starting at  $\mathbf{x}(0) = \mathbf{0} \in \mathcal{X}_0 = \{\mathbf{x} \mid |q_1| \leq \frac{\pi}{8}, |q_{2,3}| \leq \frac{\pi}{6}, |\dot{q}_{1,2,3}| \leq \frac{\pi}{6}\}$ , we consider the problem of moving the arm to the goal region  $\mathcal{X}_{\text{goal}} = \{\mathbf{x} \mid |q_1 - \frac{\pi}{2}| \leq \frac{\pi}{8}, |q_{2,3}| \leq \frac{\pi}{10}, |\dot{q}_{1,2,3}| \leq \frac{\pi}{8}\}$ . We consider two spherical obstacles  $\mathcal{O}_i \subset \mathbb{R}^3$  which should be avoided by the end-effector. This results in two obstacle avoidance constraints  $\mathbf{x} \notin \mathcal{O}_i$  written as  $\mathcal{O}_i = \{\mathbf{x} \mid \|\mathbf{p}_e(\mathbf{x}) - \mathbf{p}_i\|_2 \leq \frac{1}{4}\}$ , where  $\mathbf{p}_1 = (\frac{\sqrt{2}}{2}, -\frac{\sqrt{2}}{2}, 1.4)$ ,  $\mathbf{p}_2 = (\frac{\sqrt{2}}{2}, -\frac{\sqrt{2}}{2}, 0.6)$ , and  $\mathbf{p}_e : \mathbb{R}^3 \rightarrow \mathbb{R}^3$  maps the state  $\mathbf{x}$  to the end-effector position [65]. We also account for joint angle and velocity limits  $\mathbf{x} \in \mathcal{X}$  so that  $\mathcal{X}_{\text{free}} = \mathcal{X} \setminus (\cup_i \mathcal{O}_i)$ , with  $\mathcal{X} = \{\mathbf{x} \mid q_1 \in [-\frac{\pi}{2}, \pi], |q_{2,3}| \leq \frac{\pi}{2}, |\dot{q}_i| \leq \frac{\pi}{8}\}$ . Control bounds are set to  $\mathcal{U} = \{\mathbf{u} \mid |\tau_i| \leq 2 \text{ N}\cdot\text{m}\}$ .

We simulate (13) with an Euler discretization scheme with timestep 50 ms. To slow down the unstable dynamics of this system, we use a damping controller with approximate gravity compensation  $\mathbf{u} = \hat{N}(\mathbf{q}, \dot{\mathbf{q}}) - K_d \dot{\mathbf{q}} + \mathbf{u}_{\text{seels}}$ , where  $\hat{N}$  is computed using nominal mass and inertia values,  $K_d = [0, 4, 1]$ , and  $\mathbf{u}_{\text{seels}}$  is the open-loop control trajectory computed with our framework, where each input lasts 1 s and  $\mathbf{u}_{\text{seels}} \in \mathcal{U}$ . We use a nominal model  $\mathbf{h}$  of (13) with  $C(\mathbf{q}, \dot{\mathbf{q}}) = \mathbf{0}$  and

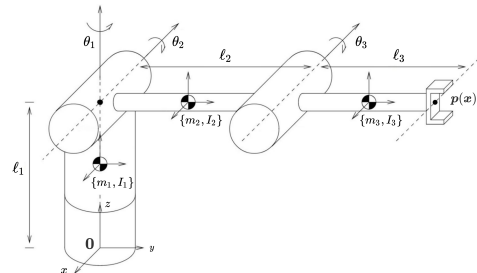


Fig. 4. Three-link open-chain manipulator, figure adapted from [65].

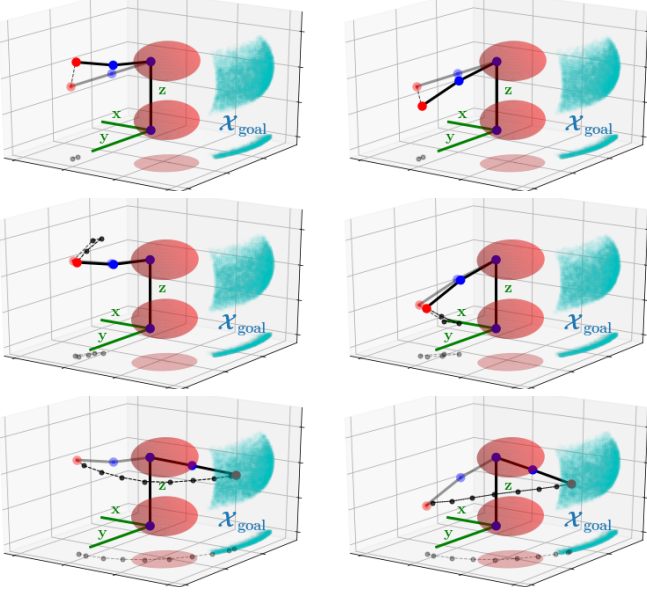


Fig. 5. Simulated manipulator experiments for a light (left) and heavy (right) arms: the robot is able to infer its dynamics through active exploration (a,b), and eventually reach  $\mathcal{X}_{\text{goal}}$  (c), while satisfying constraints at all times.

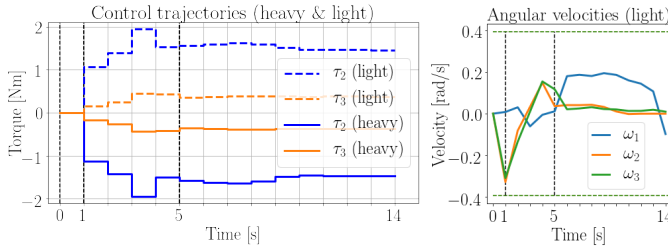


Fig. 6. Simulated manipulator experiments: control trajectories for both light and heavy manipulators (left), and angular velocities (right, light arm).

$(m_i, I_{xi} = I_{yi}, I_{zi}) = (2, 0.05, 0.01)$ . We then train an ALPACA model with  $L = 2$  layers of width 128 each and an output dimension  $d = 64$  for each  $\phi_i$ . We randomize parameters according to uniform distributions with  $m_i \in [1.75, 2.25]$  kg,  $I_{xi} = I_{yi} \in [0.04, 0.06]$  kg·m<sup>2</sup>,  $I_{zi} \in [0.008, 0.012]$  kg·m<sup>2</sup>, with  $i = 1, 2, 3$ . We assume  $\sigma_i = 10^{-3}$ , and  $|\epsilon^i| \leq (\sigma_i^2 \chi_1^2(0.95))^{1/2}$ ,  $i = 1, \dots, 6$ . We use  $\beta_i$  and orthogonality regularization,  $M = 2500$  samples for reachability analysis, and directly use our theoretically computed bounds within our safe learning algorithm, i.e., we use (5) to sample model parameters. Further details about trajectory optimizations are provided in Appendix B.

Figure 5 (left) shows the results for low mass and inertia  $(m_i, I_{xi} = I_{yi}, I_{zi}) = (1.85, 45 \cdot 10^{-3}, 8.5 \cdot 10^{-3})$ . Note that lower mass and inertia would cause the robot to leave  $\mathcal{X}_0$  in 1s, making the problem infeasible. In this experiment, the end-effector initially rises (due to the lower-than-expected mass/inertia), does a second exploration maneuver, then reaches the goal, always satisfying constraints. Figure 5 (right) shows results for a heavier arm. Again, all constraints are satisfied and the goal is reached safely. For both scenarios, we compare to a method which only considers uncertainty from the additive disturbances  $\epsilon$ , thereby deciding that directly reaching  $\mathcal{X}_{\text{goal}}$  is

safe. This naive approach fails to reach the goal and violates constraints, which demonstrates the need for an accurate model and sequential online learning to reliably solve this problem.

We plot control trajectories and angular velocities in Figure 6. This shows that steering the system with lower mass values requires less control effort, and angular velocities ( $\dot{q}_2, \dot{q}_3$ ) are larger during the second exploration phase (from  $t = 1$ s until  $t = 5$ s) in order to efficiently identify the unknown parameters of the manipulator. Also, note the approximate symmetry between the two control trajectories due to the different mass and inertial properties.

### B. Safely transporting an uncertain payload

Next, we verify our approach on a nonlinear six-dimensional planar free-flyer robot navigating in a cluttered environment. We consider the problem of cargo transport, in which the robot is attached to an uncertain payload that results in changes to the inertial properties of the system. This system mimics a cargo unloading scenario that is one plausible near-term application of autonomous robots onboard the International Space Station [40], [66].

The state of the system is given by  $\mathbf{x} = (\mathbf{p}, \theta, \mathbf{v}, \omega) \in \mathbb{R}^6$ , with  $\mathbf{p}, \mathbf{v} \in \mathbb{R}^2$  the planar position and velocity, and  $\theta, \omega \in \mathbb{R}$  the heading and angular velocity, respectively. For safety, we constrain  $|v_i| \leq 0.2$  m/s, and  $|\omega| \leq 0.25$  rad/s. The robot is controlled using two pairs of gas thrusters and a reaction wheel. The system's control inputs are denoted by  $\mathbf{u} = (F_x, F_y, M) \in \mathbb{R}^3$ , where  $\mathcal{U} = [-\bar{u}_i, \bar{u}_i]^{\times 3}$  represent the limited control authority, with  $\bar{u}_{1,2} = 0.15$  N and  $\bar{u}_3 = 0.01$  Nm. The payload causes a change in mass, inertia properties and causes the center of mass to be offset at  $\mathbf{p}_0 \in \mathbb{R}^2$ . The continuous time nonlinear dynamics of the system (which we write as  $\dot{\mathbf{x}} = \mathbf{f}_t(\cdot)$ ) are given as  $\dot{\mathbf{p}} = \mathbf{v}$ ,  $\dot{\theta} = \omega$ , and

$$m\dot{\mathbf{v}} = \mathbf{F} - \dot{\omega} \begin{bmatrix} -p_{oy} \\ p_{ox} \end{bmatrix} + \omega^2 \mathbf{p}_0, \quad J\dot{\omega} = M - p_{ox}F_y + p_{oy}F_x. \quad (14)$$

To capture payload uncertainty, we randomize the mass  $m$ , inertia  $J$ , and center of mass  $\mathbf{p}_0$  of the coupled system as

$$m \sim \text{Unif}(25, 60) \text{ kg}, \quad J \sim \text{Unif}(0.30, 0.70) \text{ kg}\cdot\text{m}^2, \\ p_{oi} \sim \text{Unif}(-7.5, 7.5) \text{ cm}, \quad i \in \{x, y\}.$$

Using a zero-order hold on the controls and a forward Euler discretization scheme, we discretize the dynamics as

$$\mathbf{x}_{t+1} = \mathbf{x}_t + \Delta t \cdot \mathbf{f}_t(\mathbf{x}_t, \mathbf{u}_t, m, \mathbf{J}, \mathbf{p}_0) + \epsilon_t, \quad (15)$$

where  $\Delta t = 3$  s and the  $\epsilon_t^i$  are  $\sigma_i$ -subgaussian, each bounded as  $|\epsilon_t^i| \leq (\sigma_i^2 \chi_1^2(0.95))^{1/2}$ , where  $\sigma_{1,2}^2 = 10^{-6}$ ,  $\sigma_{3,6}^2 = 10^{-5}$ , and  $\sigma_{4,5}^2 = 10^{-7}$ . We use this discrete time system in simulation experiments and to collect training data for offline meta-learning. We use a nominal model  $\mathbf{h}$  of the system using (15) with  $(\bar{m}, \bar{J}, \bar{\mathbf{p}}_0) = (35, 0.4, \mathbf{0})$ , which corresponds to a double-integrator model. To represent the unknown model mismatch  $\mathbf{g}(\cdot, \cdot, \xi)$ , we train an ALPACA model as described in [45] for 6000 iterations for all experiments, with  $L = 2$  layers of width 64 each and an output dimension  $d = 32$  for each  $\phi_i$ .

For trajectory optimization, we use standard linear-quadratic final and step costs on states and controls to minimize control

cost and deviation to  $\mathcal{X}_0$  or  $\mathcal{X}_{\text{goal}}$  depending on the phase. Specifically, we maximize the information cost (10) while minimizing control effort and penalizing high velocities and the final distance to  $\mathbf{x}_g$ , the center of either  $\mathcal{X}_0$ , or  $\mathcal{X}_{\text{goal}}$ :

$$\min_{\mu, \mathbf{u}} \sum_{k=0}^{N-1} \left( -\alpha_{\text{info}} \ell_{\text{info}}(\mu_k, \mathbf{u}_k) + \mu_k^T \mathbf{Q} \mu_k + \mathbf{u}_k^T \mathbf{R} \mathbf{u}_k \right) + (\mu_N - \mathbf{x}_g)^T \mathbf{Q}_N (\mu_N - \mathbf{x}_g). \quad (16)$$

We set  $\alpha_{\text{info}} = 0.025$  for exploration, whereas  $\alpha_{\text{info}} = 0$  when reaching  $\mathcal{X}_{\text{goal}}$ . We set  $\mathbf{Q} = \text{diag}([0, 0, 0, 1, 1, 10])$ ,  $\mathbf{R} = \text{diag}([10, 10, 10])$ , and  $\mathbf{Q}_N = 10^3 \text{diag}([1, 1, 0.1, 10, 10, 10])$  for both EXPLORE-OCF and REACH-OCF.

To validate our framework, we run SEELS on 250 randomized problems with different dynamics parameters  $\xi$ , four different obstacle configurations, initial and final conditions, as shown in Figure 3. With  $M = 2500$  and both orthogonality and  $\beta$ -regularization, we obtain a success rate (all constraints in (1c) are satisfied, the optimizer finds a feasible solution at each step of SEELS, and the system reaches  $\mathcal{X}_{\text{goal}}$ ) at 93.2% for  $\delta = 0.1$ , 90.5% for  $\delta = 0.2$ , and 88.8% for  $\delta = 0.5$ . This shows that the joint chance constraint (1c) is conservatively satisfied in practice and verifies the probabilistic safety and recursive feasibility results of Theorem 2.

**Sensitivity analysis:** we perform an ablation study to evaluate the sensitivity of our approach to different parameters: to  $\delta$ , to the effect of the  $\beta$ -regularizer, to the number of samples  $M$  for reachability analysis with RANDUP, and to the noise intensity  $\sigma_i$ . For each parameter set, we perform 250 randomized experiments on the environments shown in Figure 8. As with the manipulator experiments, we compare our approach with a baseline. Results are shown in Figure 7, Tables I and II, and are discussed below:

- *Baseline:* we compare with a method which only considers uncertainty from the additive disturbances  $\epsilon$ , whereby the system assumes reaching  $\mathcal{X}_{\text{goal}}$  directly is safe. This naive approach violates the joint chance constraint (1c), again demonstrating the need for uncertainty quantification and sequential active learning to reliably solve this problem.
- $\delta$ : as a consequence of Theorem 2, the algorithm’s conservatism can be tuned by the choice of  $\delta$ , which is supported by our results. In particular, by opting for a lower probability of safety  $1 - \delta$ , the goal is reached faster on average. Importantly, SEELS conservatively satisfies the joint chance constraint (1c) for these different parameters.
- $M$ : increasing  $M$  leads to increased success rate and safety probability, which is supported by the results shown in Figure 7 (right). Theoretically, under **A1-3**, success with high probability (as stated in Theorem 2) is guaranteed as long as the number of samples  $M$  is large enough (a consequence of [52, Theorem 2]), which is supported by our experiments. In practice, one should choose the largest value of  $M$  to satisfy a given computational budget and multiple techniques could be used to improve the quality of the approximation, e.g., parallelization on GPUs and importance sampling approaches [67] which we did not need in this work. We refer to [52] for further details.

Small $\sigma_i$	# Explore	$\mathbf{x} \notin \mathcal{X}_{\text{obs}}$	$\mathbf{x} \in \mathcal{X}_{\text{min/max}}$	$\mathbf{x}_N \in \mathcal{X}_{\text{goal}}$	$\mathbf{x} \in \mathcal{X}_{\text{all}}$
SEELS, $\delta=0.1$	2.3 $\pm$ 0.01	97.6 $\pm$ 1.9%	97.6 $\pm$ 1.9%	96.8 $\pm$ 2.2%	93.2 $\pm$ 3.1%
SEELS, $\delta=0.2$	2.43 $\pm$ 0.19	95.6 $\pm$ 2.5%	98.8 $\pm$ 1.3%	98.8 $\pm$ 1.3%	93.6 $\pm$ 3.0%
SEELS, $\delta=0.5$	2.22 $\pm$ 0.18	94.8 $\pm$ 2.7%	98.8 $\pm$ 1.3%	97.2 $\pm$ 2.0%	93.2 $\pm$ 3.1%
Mean-Equivalent	0	39.6 $\pm$ 6.0%	99.6 $\pm$ 0.8%	22.8 $\pm$ 5.2%	19.6 $\pm$ 4.9%

TABLE I

RESULTS FOR 250 RANDOMIZED EXPERIMENTS FOR DIFFERENT VALUES OF  $\delta$ , WITH LOW NOISE LEVELS  $\epsilon_k$ ,  $\beta$ -REG., AND  $M = 1000$ .

High $\sigma_i$	# Explore	$\mathbf{x} \notin \mathcal{X}_{\text{obs}}$	$\mathbf{x} \in \mathcal{X}_{\text{min/max}}$	$\mathbf{x}_N \in \mathcal{X}_{\text{goal}}$	$\mathbf{x} \in \mathcal{X}_{\text{all}}$
SEELS, $\delta=0.1$	2.4 $\pm$ 0.14	92.4 $\pm$ 3.3%	99.2 $\pm$ 1.1%	95.6 $\pm$ 2.5%	90.0 $\pm$ 3.7%
SEELS, $\delta=0.2$	2.32 $\pm$ 0.13	91.6 $\pm$ 3.4%	100 $\pm$ 0%	95.6 $\pm$ 2.5%	89.6 $\pm$ 3.8%
SEELS, $\delta=0.5$	1.98 $\pm$ 0.11	87.6 $\pm$ 4.1%	99.2 $\pm$ 1.1%	90.8 $\pm$ 3.6%	82.8 $\pm$ 4.7%
Mean-Equivalent	0	58.8 $\pm$ 6.1%	99.6 $\pm$ 0.8%	39.2 $\pm$ 6.0%	37.2 $\pm$ 6.0%

TABLE II

RESULTS FOR 250 RANDOMIZED EXPERIMENTS FOR DIFFERENT VALUES OF  $\delta$ , WITH HIGH NOISE LEVELS  $\epsilon_k$ ,  $\beta$ -REG., AND  $M = 2500$ .

- $\beta$ -regularization reduces conservatism while still guaranteeing probabilistic safety in practice, i.e. the model still satisfies **A2** and **A3**. Indeed, Figure 7 shows that the goal is reached faster in average and the system still conservatively satisfies (1c). This also implies that the model class with last-layer adaptation of ALPACA is expressive enough to enable meta-training of models fulfilling **A2** and **A3** with varying levels of conservatism. This could motivate future research on better meta-training of such models with different architectures and regularizers.
- $\sigma_i$ : we also consider two noise levels:
  - 1)  $\sigma_i^2 = 10^{-7}$  for  $i=1, 2, 4, 5$ , and  $\sigma_i^2 = 10^{-6}$  for  $i=3, 6$ .
  - 2)  $\sigma_i^2 = 10^{-6}$  for  $i=1, 2$ ,  $\sigma_i^2 = 10^{-5}$  for  $i=3, 6$ , and  $\sigma_i^2 = 10^{-7}$  for  $i=4, 5$ .

Results for these different noise levels for different  $\delta$  are reported in Tables I and II. From Table I, we see that the performance and overall probability of safety for small  $\sigma_i$  is not sensitive to the chosen value of  $\delta$ . We speculate that failures are mostly due to under-approximations from the approximate computation of the reachable sets with RANDUP. For higher noise levels, it is evident that the conservatism of the algorithm can be tuned by choosing a different value for  $\delta$ , since failures come from statistical errors from updating the model with noisy data (see Theorem 1). We also observe faster times to reach  $\mathcal{X}_{\text{goal}}$  when opting for lower probability of safety. In all scenarios, SEELS solves the problem with probability at least  $(1 - \delta)$ , verifying the results of Theorem 2.

## VII. HARDWARE EXPERIMENTS

Next, we verify our framework with hardware experiments. We consider the planar spacecraft free-flyer platform controlled by eight thrusters as shown in Figure 9. As the system weighs  $\sim 16\text{kg}$  and each thruster can only apply a maximum of  $0.4\text{N}$ , an accurate model and dynamically-feasible trajectory are necessary to safely reach a goal region. Other challenges include imperfect actuators, time-varying mass of the system as the gas tanks deplete, and unmodeled friction and tilt of the



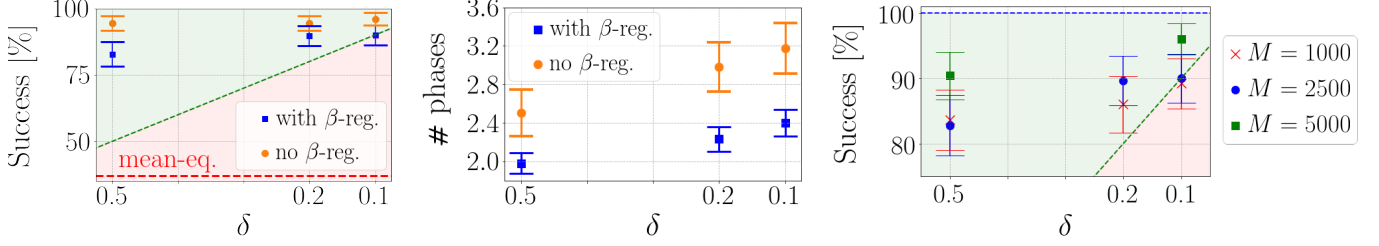


Fig. 7. Simulation results for ablation study, using 250 free-flyer experiments in randomized environments (see Fig. 8) with high noise levels  $\sigma_i$ , with and without  $\beta$ -regularization (top figures, using  $M = 2500$ ) and for different number values of  $M$  (bottom). On plots showing success percentages (all constraints are satisfied and  $\mathbf{x}_N \in \mathcal{X}_{\text{goal}}$ ), the green region denotes results where the success percentage is at or above the desired probability of success given by  $\delta$ , and the red region indicates where the true probability of success is lower than desired. Error bars correspond to 95% confidence intervals.

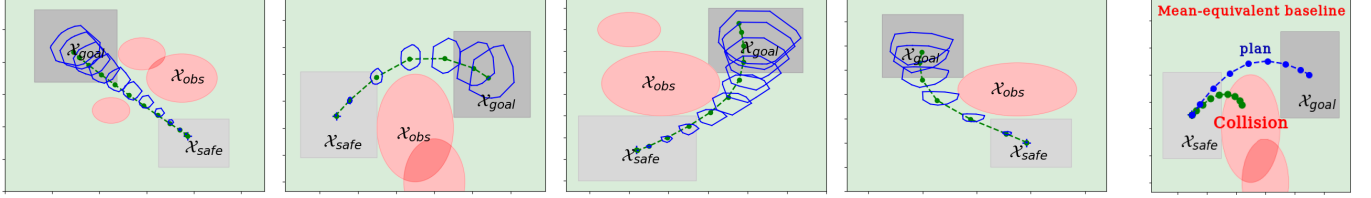


Fig. 8. **Left** four figures: scenarios considered for the ablation study with representative reaching trajectories obtained with SEELS and true executed trajectories. **Right**, mean-equivalent baseline: due to high uncertainty, attempting to reach  $\mathcal{X}_{\text{goal}}$  is initially unsafe, violating velocity and final constraints, and colliding with an obstacle.

table surface. Our implementation follows Section VI-B (with  $\delta=0.1$ , orthogonality and  $\beta$ -regularization) with the following modifications:

- *Dynamics*: we meta-train using (14) discretized at 10Hz with an additional random force  $\mathbf{F}_{\text{tilt}}$  for the tilt of the table. For offline meta-training, the parameters are randomized as

$$m \sim \text{Unif}(8, 40) \text{ kg}, \quad J \sim \text{Unif}(0.08, 0.30) \text{ kg}\cdot\text{m}^2, \\ p_{oi} \sim \text{Unif}(\pm 5) \text{ cm}, \quad F_{\text{tilt},i} \sim \text{Unif}(\pm 0.3) \text{ N}, \quad i \in \{x, y\}.$$

- *Regulation*: we regulate the system with a PD controller (see A1) at the end of each phase as a new plan is computed. We do not use these intermediate trajectories to learn dynamics.
- *Feedback*: we use a LQR controller to stabilize the trajectory around each reachable set center  $\mu_k$  and reduce uncertainty. We account for this controller during planning as in [27] and apply the control  $\mathbf{u}_k = \mathbf{u}_{\text{seels},k} + \text{LQR}(\mathbf{x}_k - \mu_k)$  at  $\frac{1}{3}$  Hz.

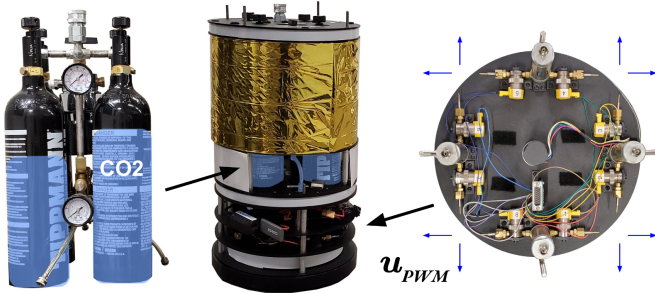


Fig. 9. The free-flyer robot uses air bearings and cold-gas thrusters to navigate with minimal friction and external forces on a smooth, flat granite table, emulating microgravity dynamics within a plane. **Right** (top view): The eight cold-gas thrusters are mixed to produced desired forces and moments on the robot, modulated using 10 Hz PWM signals sent to the thruster valves. The lack of reaction wheel on this system makes it slightly more challenging to control than the simulated free-flyer from Section VI-B.

We use a motion capture system and interface our Python implementation with ROS. Using SEELS, we compute a desired wrench  $\mathbf{u} = [F_x, F_y, M]$  in the world frame, which we then convert to the local frame of the robot, yielding  $\mathbf{u}_{\text{body}}$ . We then translate these forces and torque into corresponding PWM signals for the actuators:

$$\mathbf{u}_{\text{PWM}} = \text{saturate}(\mathbf{A}\mathbf{u}_{\text{body}}) \in \mathbb{R}^8.$$

The constant matrix  $\mathbf{A} \in \mathbb{R}^{8 \times 3}$  accounts for the maximum applicable force of each thruster of 0.4N. With the control bounds for planning set conservatively to  $|F_{x,y}| \leq 0.4\text{N}$  and  $|M| \leq 0.03\text{Nm}$ , we can ensure that actuator saturation will neither occur during exploration nor exploitation.

This approach of using a lower-level control mapping to turn world-frame forces and torques to gas-thruster commands allows us to use the same dynamics model used in the simulation experiments (Section VI) for the hardware experiments (retraining it to also account for the slight tilt of the table). An alternative would be to learn a dynamics model in terms of gas-thruster inputs directly. While this modeling choice would allow factoring in dynamics uncertainty at the actuator level (e.g., actuator failure), this would also yield a more complex class of possible models and thus require a larger model to ensure Assumption 2 on model capacity is still satisfied.

With these modifications, we apply SEELS on multiple obstacle fields and analyze the representative experiment in Figure 10. Initially, uncertainty is too large to safely reach  $\mathcal{X}_{\text{goal}}$  and REACH-OCF is infeasible. Instead, the agent performs a short exploration trajectory with negligible control inputs to first infer the tilt of the table (EXPLORE-OCF is necessarily feasible for a planning horizon short enough, see Theorem 2). Indeed, applying larger control inputs would yield larger reachable sets (due to inertial uncertainty) and violate constraints. Then, SEELS still deems reaching to be unsafe

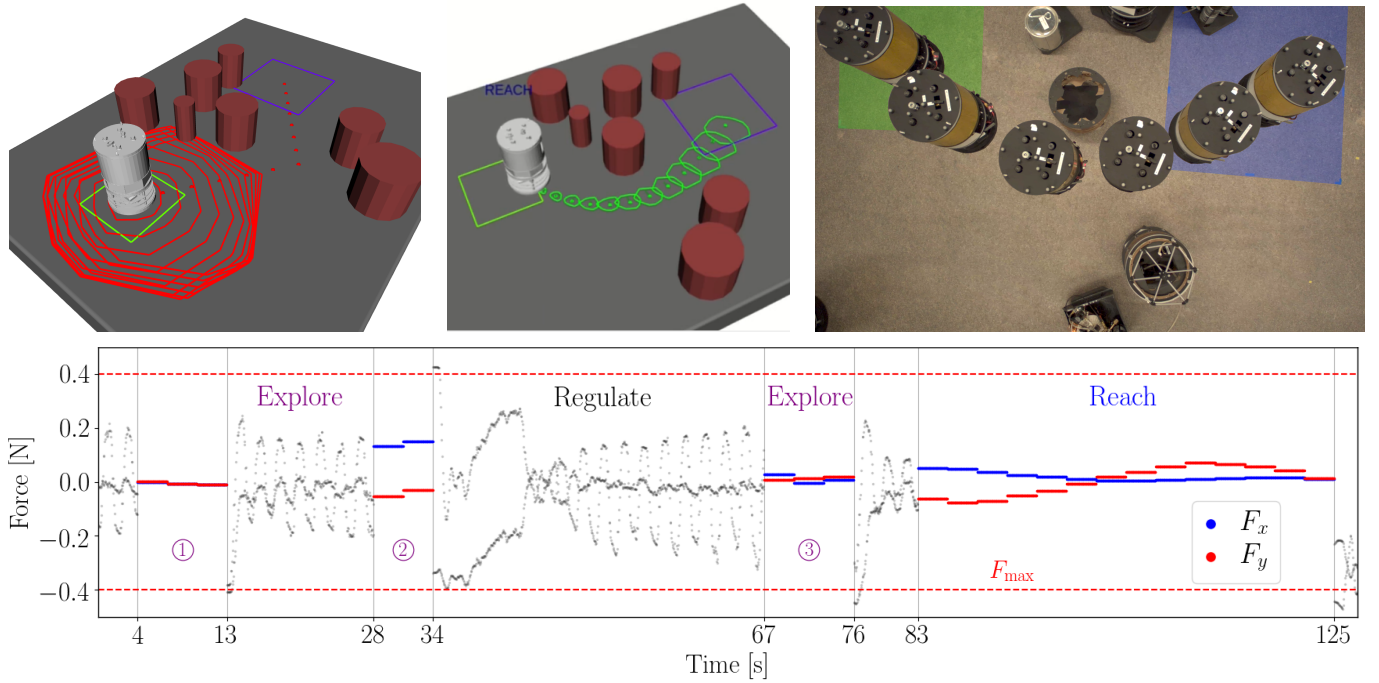


Fig. 10. Visualization and forces applied during hardware experiment. **Top (left) & bottom (1)**: uncertainty is too high to reach and an exploration trajectory with negligible control inputs is computed to infer external forces. **Bottom (2) and (3)**: uncertainty is still too high and larger forces are computed to infer inertial properties. **Top (middle, right) & bottom**: the goal is safely reached.

and thus performs two additional exploration trajectories to infer the inertial properties of the system. Once REACH-OCF is feasible, the robot finally reaches the goal. All constraints are satisfied throughout the experiment.

We present further results in the attached video available at <https://youtu.be/bvG-g3NADUc> and summarize them as follows:

- *Baseline*: we compare with a mean-equivalent approach which collides with obstacles despite the LQR controller. This shows that considering uncertainty during planning and learning the dynamics is necessary to reliably solve this task.
- *Reliability*: our approach works repeatably in multiple obstacle fields, including a payload-grasping experiment. We also present two experiments where the agent infers its dynamics, reaches a first goal, and is then capable of reaching another destination directly without needing further exploration. All constraints are satisfied throughout the experiments: Theorem 2 can easily be extended to also guarantee the success of such multi-setpoint problems.
- *Failure modes* are also discussed. We observed that failures to reach  $\mathcal{X}_{\text{goal}}$  are either due to (1) the model adapting incorrectly during the initial exploration phases due to noisy measurements and sim-to-real mismatch, resulting in large variations in the parameters  $\theta_i$ , which is easy to detect and could be addressed by re-initializing parameters based on the variances  $\sigma_i \Lambda_i^{-1}$  or by increasing  $\sigma_i$  to learn less rapidly, (2) infeasible trajectory optimization, or (3) gas tanks that are too depleted to apply desired forces. In these situations, we observed that no feasible trajectory to the goal is found and the algorithm defaults to exploring safely within  $\mathcal{X}_0$ .

## VIII. CONCLUSION

To safely perform tasks under high initial uncertainty, we presented a framework to sequentially explore and learn the properties of a dynamical system while guaranteeing safety at all times as a single joint chance constraint. We demonstrated our approach through simulations and hardware experiments, where we showed that a free-flying robot emulating a spacecraft can reliably infer its dynamics and safely reach a goal.

*Future work.* Problems with time-varying dynamics (e.g., the system is attached to a new payload during operation and gas tanks are depleting) could be addressed using continual meta-learning approaches [68], which would require a new analysis to guarantee safety. Future work could also derive algorithms to compute invariant sets satisfying **A1** by leveraging the prior of the meta-learning model. Extensions of [52] would strengthen the safety guarantees to the case of a finite number of samples for uncertainty propagation and work on free-final-time trajectory optimization would replace the search over horizons  $N$  in our algorithm. Investigating regret bounds for such constrained problems would also help provide guarantees on the time required to perform a task given known geometric properties of the problem. Finally, our framework could be combined with existing learning-based controllers to improve performance.

## ACKNOWLEDGMENTS

This work was supported in part by NASA under the University Leadership Initiative (Grant #80NSSC20M0163) and the Early Stage Innovations program, by the Office of Naval Research YIP program, and by DARPA under the

Assured Autonomy program. This article solely reflects the opinions and conclusions of its authors.

## REFERENCES

- [1] B. Recht, “A tour of reinforcement learning: The view from continuous control,” *Annual Review of Control, Robotics, and Autonomous Systems*, vol. 2, no. 1, pp. 253–279, 2019.
- [2] M. Deisenroth, D. Fox, and C. Rasmussen, “Gaussian processes for data-efficient learning in robotics and control,” *IEEE Transactions on Pattern Analysis & Machine Intelligence*, vol. 37, no. 2, pp. 408–423, 2015.
- [3] S. Levine, C. Finn, T. Darrell, and P. Abbeel, “End-to-end training of deep visuomotor policies,” *Journal of Machine Learning Research*, vol. 17, pp. 1–40, 2016.
- [4] J. Coulson, J. Lygeros, and F. Dörfler, “Data-enabled predictive control: In the shallows of the DeePC,” in *European Control Conference*, 2019.
- [5] —, “Distributionally robust chance constrained data-enabled predictive control,” in *Proc. IEEE Conf. on Decision and Control*, 2019.
- [6] J. Berberich, J. Köhler, M. A. Müller, and F. Allgöwer, “Robust constraint satisfaction in data-driven MPC,” in *Proc. IEEE Conf. on Decision and Control*, 2020.
- [7] —, “Data-driven model predictive control with stability and robustness guarantees,” *IEEE Transactions on Automatic Control*, pp. 1–1, 2020.
- [8] J.-J. E. Slotine and W. Li, “On the adaptive control of robot manipulators,” *Int. Journal of Robotics Research*, vol. 6, no. 3, pp. 49–59, 1987.
- [9] B. T. Lopez and J.-J. E. Slotine, “Adaptive nonlinear control with contraction metrics,” *IEEE Control Systems Letters*, vol. 5, no. 1, pp. 205–210, 2021.
- [10] H. Mania, M. I. Jordan, and B. Recht. (2020) Active learning for nonlinear system identification with guarantees. Available at <https://arxiv.org/abs/2006.10277>.
- [11] S. Kakade, A. Krishnamurthy, K. Lowrey, M. Ohnishi, and W. Sun, “Information theoretic regret bounds for online nonlinear control,” in *Conf. on Neural Information Processing Systems*, 2020.
- [12] G. Shi, X. Shi, M. O’Connell, R. Yu, K. Azizzadenesheli, A. Anandkumar, Y. Yue, and S.-J. Chung, “Neural lander: Stable drone landing control using learned dynamics,” in *Proc. IEEE Conf. on Robotics and Automation*, 2019.
- [13] J. Schmidhuber, “Evolutionary principles in self-referential learning, or on learning how to learn: the meta-meta-... hook,” Ph.D. dissertation, Technische Universität München, 1987.
- [14] A. Santoro, S. Bartunov, M. Botvinick, D. Wierstra, and T. Lillicrap, “Meta-learning with memory-augmented neural networks,” in *Int. Conf. on Machine Learning*, 2016.
- [15] C. Finn, P. Abbeel, and S. Levine, “Model-agnostic meta-learning for fast adaptation of deep networks,” in *Int. Conf. on Machine Learning*, 2017.
- [16] A. Nagabandi, I. Clavera, L. Simin, R. S. Fearing, P. Abbeel, S. Levine, and C. Chelsea Finn, “Learning to adapt in dynamic real-world environments through meta-reinforcement learning,” in *Int. Conf. on Learning Representations*, 2019.
- [17] S. Belkale, R. Li, G. Kahn, R. McAllister, R. Calandra, and S. Levine, “Model-based meta-reinforcement learning for flight with suspended payloads,” *IEEE Robotics and Automation Letters*, 2021, to appear.
- [18] J. Harrison, A. Sharma, and M. Pavone, “Meta-learning priors for efficient online bayesian regression,” in *Workshop on Algorithmic Foundations of Robotics*, 2018.
- [19] C. Williams and C. E. Rasmussen, *Gaussian processes for machine learning*. MIT press, 2006.
- [20] C. Fiedler, C. W. Scherer, and S. Trimpe. (2021) Practical and rigorous uncertainty bounds for gaussian process regression. Available at <https://arxiv.org/abs/2105.02796>.
- [21] F. Berkenkamp, M. Turchetta, A. Schoellig, and A. Krause, “Safe model-based reinforcement learning with stability guarantees,” in *Conf. on Neural Information Processing Systems*, 2017.
- [22] T. Koller, F. Berkenkamp, M. Turchetta, and A. Krause, “Learning-based model predictive control for safe exploration,” in *Proc. IEEE Conf. on Decision and Control*, 2018.
- [23] Y. Abbasi-Yadkori, D. Pál, and C. Szepesvári, “Improved algorithms for linear stochastic bandits,” in *Conf. on Neural Information Processing Systems*, 2011.
- [24] L. Hewing, J. Kabzan, and M. N. Zeilinger, “Cautious Model Predictive Control using Gaussian Process Regression,” *IEEE Transactions on Control Systems Technology*, vol. 28, no. 6, 2020.
- [25] B. Ivanovic and M. Pavone, “The Trajectron: Probabilistic multi-agent trajectory modeling with dynamic spatiotemporal graphs,” in *IEEE Int. Conf. on Computer Vision*, 2019, pp. 2375–2384.
- [26] M. Castillo-Lopez, S. A. Ludvig, P. Sajadi-Alamdari, J. L. Sanchez-Lopez, M. A. Olivares-Mendez, and H. Voos, “A real-time approach for chance-constrained motion planning with dynamic obstacles,” *IEEE Robotics and Automation Letters*, vol. 5, no. 2, pp. 3620 – 3625, 2019.
- [27] T. Lew, R. Bonalli, and M. Pavone, “Chance-constrained sequential convex programming for robust trajectory optimization,” in *European Control Conference*, 2020.
- [28] K. Polymenakos, L. Laurenti, A. Patane, J. P. Calliess, L. Cardelli, M. Kwiatkowska, A. Abate, and S. Roberts, “Safety guarantees for planning based on iterative Gaussian processes,” in *Proc. IEEE Conf. on Decision and Control*, 2020.
- [29] M. J. Khojasteh, V. Dhiman, M. Franceschetti, and N. Atanasov, “Probabilistic safety constraints for learned high relative degree system dynamics,” in *2nd Annual Conference on Learning for Dynamics & Control*, 2020.
- [30] R. Cheng, M. J. Khojasteh, A. D. Ames, and J. W. Burdick, “Safe multi-agent interaction through robust control barrier functions with learned uncertainties,” in *Proc. IEEE Conf. on Decision and Control*, 2020.
- [31] K. M. Frey, T. J. Steiner, and J. P. How, “Collision probabilities for continuous-time systems without sampling,” in *Robotics: Science and Systems*, 2020.
- [32] E. Schmerling and M. Pavone, “Evaluating trajectory collision probability through adaptive importance sampling for safe motion planning,” in *Robotics: Science and Systems*, 2017.
- [33] L. Blackmore, M. Ono, and B. C. Williams, “Chance-constrained optimal path planning with obstacles,” *IEEE Transactions on Robotics*, vol. 27, no. 6, pp. 1080–1094, 2011.
- [34] J. Hwangbo, J. Lee, A. Dosovitskiy, D. Bellicoso, V. Tsounis, V. Koltun, and M. Hutter, “Learning agile and dynamic motor skills for legged robots,” *Science Robotics*, vol. 4, no. 26, 2019.
- [35] F. Berkenkamp, “Safe exploration in reinforcement learning: Theory and applications in robotics,” Ph.D. dissertation, Institute for Machine Learning, ETH Zürich, 2018.
- [36] Y. Chow, O. Nachum, A. Faust, E. Duenez-Guzman, and M. Ghavamzadeh. (2020) Safe policy learning for continuous control. Available at <https://openreview.net/pdf?id=HkxeThNFPH>.
- [37] T. Lew, A. Sharma, J. Harrison, and M. Pavone, “Safe learning and control using meta-learning,” in *Robotics: Science and Systems, Workshop on Robust Autonomy*, 2019.
- [38] Y. N. Nakka, A. Liu, G. Shi, A. Anandkumar, Y. Yue, and S. J. Chung, “Chance-constrained trajectory optimization for safe exploration and learning of nonlinear systems,” *IEEE Robotics and Automation Letters*, vol. 6, no. 2, pp. 389–396, 2020.
- [39] T. Lew, A. Sharma, J. Harrison, and M. Pavone, “On the problem of reformulating systems with uncertain dynamics as a stochastic differential equation,” 2021, available at <http://asl.stanford.edu/wp-content/papercite-data/pdf/dynSDE.pdf>.
- [40] M. Ekal and R. Ventura, “On the accuracy of inertial parameter estimation of a free-flying robot while grasping an object,” *Journal of Intelligent & Robotic Systems*, pp. 1–11, 2019.
- [41] W. Zhang, M. Tognon, L. Ott, R. Siegwart, and J. Nieto, “Active model learning using informative trajectories for improved closed-loop control on real robots,” in *Proc. IEEE Conf. on Robotics and Automation*, 2021.
- [42] E. D. Klenke and P. Hennig, “Dual control for approximate Bayesian reinforcement learning,” *Journal of Machine Learning Research*, vol. 17, no. 1, pp. 1–30, 2016.
- [43] E. Arcari, L. Hewing, and M. N. Zeilinger. (2019) An approximate dynamic programming approach for dual stochastic model predictive control. Available at <http://arxiv.org/abs/1911.03728>.
- [44] G. P. and F. Wyszotzki, “Risk-sensitive reinforcement learning applied to control under constraints,” *Journal of Artificial Intelligence Research*, vol. 34, pp. 81–108, 2020.
- [45] J. Harrison, A. Sharma, R. Calandra, and M. Pavone, “Control adaptation via meta-learning dynamics,” in *NeurIPS Workshop on Meta-Learning*, 2018.
- [46] S. Hochreiter, A. S. Younger, and P. R. Conwell, “Learning to learn using gradient descent,” in *International Conference on Artificial Neural Networks*, 2001.
- [47] J. Snoek, O. Rippel, K. Swersky, N. Satish, N. Sundaram, M. M. A. Patwary, P. Prabhat, and R. P. Adams, “Scalable bayesian optimization using deep neural networks,” in *Int. Conf. on Learning Representations*, 2015.

- [48] V. Kuleshov, N. Fenner, and S. Ermon, “Accurate uncertainties for deep learning using calibrated regression,” in *Int. Conf. on Machine Learning*, 2018.
- [49] K. Jia, S. Li, Y. Wen, T. Liu, and D. Tao, “Orthogonal deep neural networks,” *IEEE Transactions on Pattern Analysis & Machine Intelligence*, 2020.
- [50] S. Banerjee, J. Harrison, P. M. Furlong, and M. Pavone, “Adaptive meta-learning for identification of rover-terrain dynamics,” in *Int. Symp. on Artificial Intelligence, Robotics and Automation in Space*, 2020.
- [51] W. H. Greene, *Econometric Analysis*, 5th ed. Prentice Hall, 2002.
- [52] T. Lew and M. Pavone, “Sampling-based reachability analysis: A random set theory approach with adversarial sampling,” in *Conf. on Robot Learning*, 2020.
- [53] S. Singh, Y.-L. Chow, A. Majumdar, and M. Pavone, “A framework for time-consistent, risk-sensitive model predictive control: Theory and algorithms,” *IEEE Transactions on Automatic Control*, vol. 64, no. 7, pp. 2905–2912, 2018.
- [54] Y. Bar-Shalom and E. Tse, “Dual effect, certainty equivalence, and separation in stochastic control,” *IEEE Transactions on Automatic Control*, vol. 19, no. 5, 1974.
- [55] D. J. C. MacKay, “Information-based objective functions for active data selection,” *Neural Computation*, vol. 4, no. 4, pp. 590–604, 1992.
- [56] N. Srinivas, A. Krause, S. Kakade, and M. Seeger, “Gaussian process optimization in the bandit setting: No regret and experimental design,” in *Int. Conf. on Machine Learning*, 2010.
- [57] A. Chowdhury, S. R. Gopalan, “On kernelized multi-armed bandits,” in *Int. Conf. on Machine Learning*, 2017.
- [58] M. Ono, “Joint chance-constrained model predictive control with probabilistic resolvability,” in *American Control Conference*, 2012.
- [59] S. Bansal, S. L. Chen, M. Herbert, and C. J. Tomlin, “Hamilton-Jacobi reachability: A brief overview and recent advances,” in *Proc. IEEE Conf. on Decision and Control*, 2017.
- [60] D. D. Fan, A. Agha-mohammadi, and E. A. Theodorou, “Deep learning tubes for tube MPC,” in *Robotics: Science and Systems*, 2020.
- [61] R. Ivanov, J. Weimer, R. Alur, G. J. Pappas, and I. Lee, “Verisig: verifying safety properties of hybrid systems with neural network controllers,” in *Hybrid Systems: Computation and Control*, 2019.
- [62] Y. Mao, M. Szmuk, and B. Açikmeşe, “Successive convexification of non-convex optimal control problems and its convergence properties,” in *Proc. IEEE Conf. on Decision and Control*, 2016.
- [63] R. Bonalli, A. Cauligi, A. Bylard, and M. Pavone, “GuSTO: guaranteed sequential trajectory optimization via sequential convex programming,” in *Proc. IEEE Conf. on Robotics and Automation*, 2019.
- [64] B. Stellato, G. Banjac, P. Goulart, A. Bemporad, and S. Boyd, “OSQP: An operator splitting solver for quadratic programs,” 2017, Available at <https://arxiv.org/abs/1711.08013>.
- [65] R. Murray, S. S. Sastry, and L. Zexiang, *A Mathematical Introduction to Robotic Manipulation*. CRC Press, 1994.
- [66] L. Fluckiger, K. Browne, B. Coltin, J. Fusco, T. Morse, and A. Symington, “Astrobee robot software: Enabling mobile autonomy on the ISS,” in *Int. Symp. on Artificial Intelligence, Robotics and Automation in Space*, 2018.
- [67] G. Williams, N. Wagener, B. Goldfain, P. Drews, J. M. Rehg, B. Boots, and E. A. Theodorou, “Information theoretic mpc for model-based reinforcement learning,” in *Proc. IEEE Conf. on Robotics and Automation*, 2017.
- [68] J. Harrison, A. Sharma, C. Finn, and M. Pavone, “Continuous meta-learning without tasks,” in *Conf. on Neural Information Processing Systems*, 2020.

## APPENDIX

### A. Proof of Theorem 1

The proof of Theorem 1 follows from the proof of [23, Theorem 2], by making substitutions accordingly for our meta-learning model. To do so, we use the following lemma, which follows from [23, Theorem 1], by considering each dimension  $i = 1, \dots, n$  of the meta-learning model independently.

**Lemma 1** (Self-Normalized Bound for Vector-Valued Martingales). *Let  $\{\mathcal{F}_t\}_{t=0}^\infty$  be a filtration. Define  $\{\epsilon_t^i\}_{t=1}^\infty$ , a real-valued stochastic process such that  $\epsilon_t^i$  is  $\mathcal{F}_t$ -measurable, and*

*conditionally  $\sigma_i$ -subgaussian. Let  $\{\phi_t\}_{t=1}^\infty$  be a  $\mathbb{R}^d$ -valued stochastic process such that  $\phi_t$  is  $\mathcal{F}_{t-1}$ -measurable.*

*Let  $\Lambda_{i,0}$  be a  $d \times d$  positive definite matrix, and define  $\Lambda_{i,t}$  as in (3). Further, for any  $t \geq 0$ , define  $\mathbf{S}_t = \sum_{s=1}^t \epsilon_s^i \phi_s$ . Then, for any  $\delta_i > 0$ , with probability at least  $(1 - \delta_i)$*

$$\|\mathbf{S}_t\|_{\Lambda_{i,t}^{-1}}^2 \leq 2\sigma_i^2 \log \left( \frac{1}{\delta_i} \frac{\det(\Lambda_{i,t})^{1/2}}{\det(\Lambda_{i,0})^{1/2}} \right) \quad \forall t \geq 0. \quad (17)$$

*Proof.* The filtration  $\{\mathcal{F}_t\}_{t=0}^\infty$  is defined by considering the  $\sigma$ -algebra  $\mathcal{F}_t = \sigma(\phi_1, \dots, \phi_{t+1}, \epsilon_0, \dots, \epsilon_t)$ , where  $\phi_t = \phi(\mathbf{x}_t, \mathbf{u}_t)$ , and the  $\mathbf{x}_t$  are given by (1b). Then, this result follows by direct application of [23, Theorem 1], substituting  $(X, \eta, \theta, \bar{V}, V)$  with  $(\phi, \epsilon^i, \theta_i, \Lambda_{i,t}, \Lambda_{i,0})$ .  $\square$

We stress that (17) holds jointly for all times  $t \geq 0$ , such that  $\mathbb{P}((17)) \geq (1 - \delta_i)$ . This result is key to ensure joint chance constraint satisfaction, and guarantee safety and feasibility of our framework. Next, we restate and prove Theorem 1.

**Theorem 1** (Uniformly Calibrated Confidence Sets). *Consider the true system (1b),*

$$\mathbf{x}_{t+1} = \mathbf{h}(\mathbf{x}_t, \mathbf{u}_t) + \mathbf{g}(\mathbf{x}_t, \mathbf{u}_t, \boldsymbol{\xi}) + \boldsymbol{\epsilon}_t,$$

*where each  $\epsilon_t^i$  is  $\sigma_i$ -subgaussian and bounded ( $\epsilon_t^i \in \mathcal{E}_i$ ). Consider the meta-learning model given as  $\hat{g}_i(\mathbf{x}, \mathbf{u}) = \theta_i \phi_i(\mathbf{x}, \mathbf{u})$ , where  $\phi_i : \mathbb{R}^n \times \mathbb{R}^m \rightarrow \mathbb{R}^d$ ,  $\theta_i \in \mathbb{R}^d$ , and  $i = 1, \dots, n$ . Starting from  $(\bar{\theta}_{i,0}, \Lambda_{i,0})$ , with  $\bar{\theta}_{i,0} \in \mathbb{R}^d$ , and  $\Lambda_{i,0}$  is a  $d \times d$  positive definite matrix, define the sequence  $\{(\bar{\theta}_{i,s}, \Lambda_{i,s})\}_{s=0}^t$ , where  $(\bar{\theta}_{i,t}, \Lambda_{i,t})$  is computed with online data from (1b) using (3):*

$$\begin{aligned} \Lambda_{i,t} &= \Phi_{i,t-1}^\top \Phi_{i,t-1} + \Lambda_{i,0}, \\ \bar{\theta}_{i,t} &= \Lambda_{i,t}^{-1} (\Phi_{i,t-1}^\top \mathbf{G}_{i,t} + \Lambda_{i,0} \bar{\theta}_{i,0}), \end{aligned} \quad i = 1, \dots, n,$$

*where  $\mathbf{G}_{i,t}^\top = [x_{i,1} - h_i(\mathbf{x}_0, \mathbf{u}_0), \dots, x_{i,t} - h_i(\mathbf{x}_{t-1}, \mathbf{u}_{t-1})] \in \mathbb{R}^t$ , and  $\Phi_{i,t-1}^\top = [\phi_i(\mathbf{x}_0, \mathbf{u}_0), \dots, \phi_i(\mathbf{x}_{t-1}, \mathbf{u}_{t-1})] \in \mathbb{R}^{d \times t}$ . Further, define  $\delta_i = \delta/(2n)$ , and let*

$$\begin{aligned} \beta_{i,t}^\delta &= \sigma_i \left( \sqrt{2 \log \left( \frac{1}{\delta_i} \frac{\det(\Lambda_{i,t})^{1/2}}{\det(\Lambda_{i,0})^{1/2}} \right)} + \sqrt{\frac{\bar{\lambda}(\Lambda_{i,0})}{\bar{\lambda}(\Lambda_{i,t})} \chi_d^2(1 - \delta_i)} \right), \\ \text{and } \mathcal{C}_{i,t}^\delta(\bar{\theta}_{i,t}, \Lambda_{i,t}) &= \{\theta_i \mid \|\theta_i - \bar{\theta}_{i,t}\|_{\Lambda_{i,t}} \leq \beta_{i,t}^\delta\}. \end{aligned}$$

*Then, under Assumptions 2 and 3,*

$$\mathbb{P}(\theta_i^* \in \mathcal{C}_{i,t}^\delta(\bar{\theta}_{i,t}, \Lambda_{i,t}) \quad \forall t \geq 0) \geq (1 - 2\delta_i).$$

*Proof.* This proof is a straightforward extension of [23, Theorem 2], where we use Assumption 3 to provide a probabilistic error bound for the model mismatch over the prior for  $\theta_i^*$ , Lemma 1 to bound the estimation error due to  $\epsilon_t$ , and Boole's inequality to obtain  $\beta_i$ .

Define  $\epsilon^i = (\epsilon_1^i, \dots, \epsilon_t^i)^\top$ . For conciseness, we drop the indices  $i$  and  $t$ , and denote  $(\theta^*, \bar{\theta}, \Lambda, \bar{\theta}_0, \Lambda_0, \Phi, \epsilon) = (\theta_i^*, \bar{\theta}_{i,t}, \Lambda_{i,t}, \bar{\theta}_{i,0}, \Lambda_{i,0}, \Phi_{i,t-1}, \epsilon^i)$ . Under Assumption 2, we can write  $\mathbf{G}_{i,t} = \Phi \theta^* + \epsilon$ . Then, we rewrite the mean estimate  $\bar{\theta}$  of  $\theta^*$  at time  $t$  as

$$\begin{aligned} \bar{\theta} &= (\Lambda_0 + \Phi^\top \Phi)^{-1} (\Lambda_0 \bar{\theta}_0 + \Phi^\top (\Phi \theta^* + \epsilon)) \\ &= (\Lambda_0 + \Phi^\top \Phi)^{-1} \Phi^\top \epsilon + (\Lambda_0 + \Phi^\top \Phi)^{-1} (\Lambda_0 + \Phi^\top \Phi) \theta^* \\ &\quad - (\Lambda_0 + \Phi^\top \Phi)^{-1} \Lambda_0 (\theta^* - \bar{\theta}_0) \\ &= \Lambda^{-1} \Phi^\top \epsilon + \theta^* - \Lambda^{-1} \Lambda_0 (\theta^* - \bar{\theta}_0), \end{aligned}$$



from which we obtain, for any  $\mathbf{a} \in \mathbb{R}^d$ , that  $\mathbf{a}^T(\bar{\boldsymbol{\theta}} - \boldsymbol{\theta}^*) = \mathbf{a}^T(\Lambda^{-1}\Phi^T\boldsymbol{\epsilon}) - \mathbf{a}^T(\Lambda^{-1}\Lambda_0(\boldsymbol{\theta}^* - \bar{\boldsymbol{\theta}}_0))$ . With this result, by the Cauchy-Schwarz inequality,

$$|\mathbf{a}^T(\bar{\boldsymbol{\theta}} - \boldsymbol{\theta}^*)| \leq \|\mathbf{a}\|_{\Lambda_t^{-1}} (\|\Phi^T\boldsymbol{\epsilon}\|_{\Lambda^{-1}} + \|\Lambda_0(\boldsymbol{\theta}^* - \bar{\boldsymbol{\theta}}_0)\|_{\Lambda^{-1}}) \\ \leq \|\mathbf{a}\|_{\Lambda^{-1}} \left( \|\Phi^T\boldsymbol{\epsilon}\|_{\Lambda^{-1}} + \sqrt{\frac{\bar{\lambda}(\Lambda_0)}{\bar{\lambda}(\Lambda)}} \|\boldsymbol{\theta}^* - \bar{\boldsymbol{\theta}}_0\|_{\Lambda_0} \right), \quad (18)$$

where the second inequality is obtained as

$$\|\Lambda_0(\boldsymbol{\theta}^* - \bar{\boldsymbol{\theta}}_0)\|_{\Lambda^{-1}}^2 \leq \frac{\bar{\lambda}(\Lambda^{-1})}{\bar{\lambda}(\Lambda_0^{-1})} \|\Lambda_0(\boldsymbol{\theta}^* - \bar{\boldsymbol{\theta}}_0)\|_{\Lambda_0^{-1}}^2 \\ = \frac{\bar{\lambda}(\Lambda_0)}{\bar{\lambda}(\Lambda)} \|\Lambda_0(\boldsymbol{\theta}^* - \bar{\boldsymbol{\theta}}_0)\|_{\Lambda_0^{-1}}^2 = \frac{\bar{\lambda}(\Lambda_0)}{\bar{\lambda}(\Lambda)} \|\boldsymbol{\theta}^* - \bar{\boldsymbol{\theta}}_0\|_{\Lambda_0}^2.$$

By Lemma 1, for any  $\delta_i$ , with probability at least  $(1 - \delta_i)$ ,

$$\|\Phi^T\boldsymbol{\epsilon}\|_{\Lambda^{-1}}^2 \leq 2\sigma_i^2 \log \left( \frac{1}{\delta_i} \frac{\det(\Lambda)^{1/2}}{\det(\Lambda_0)^{1/2}} \right) \quad \forall t \geq 0 \quad (19)$$

By Assumption 3, for  $\delta_i = \delta/(2n)$ , with probability at least  $(1 - \delta_i)$ ,

$$\|\boldsymbol{\theta}^* - \bar{\boldsymbol{\theta}}_0\|_{\Lambda_0}^2 \leq \sigma_i^2 \chi_d^2 (1 - \delta_i). \quad (20)$$

From (18), by Boole's inequality<sup>7</sup>, we have that with probability at least  $(1 - 2\delta_i)$ , for all  $t \geq 0$ , and any  $\mathbf{a} \in \mathbb{R}^d$ ,

$$|\mathbf{a}^T(\bar{\boldsymbol{\theta}} - \boldsymbol{\theta}^*)| \leq \|\mathbf{a}\|_{\Lambda^{-1}} \sigma_i \left( \sqrt{2 \log \left( \frac{1}{\delta_i} \frac{\det(\Lambda)^{1/2}}{\det(\Lambda_0)^{1/2}} \right)} \right. \\ \left. + \sqrt{\frac{\bar{\lambda}(\Lambda_0)}{\bar{\lambda}(\Lambda)}} \chi_d^2 (1 - \delta_i) \right).$$

Define  $\beta_{i,t}^\delta$  as in (5). Then, letting  $\mathbf{a} = \Lambda(\bar{\boldsymbol{\theta}} - \boldsymbol{\theta}^*)$  in the expression above, we obtain

$$\|\bar{\boldsymbol{\theta}} - \boldsymbol{\theta}^*\|_{\Lambda}^2 \leq \|\Lambda(\bar{\boldsymbol{\theta}} - \boldsymbol{\theta}^*)\|_{\Lambda^{-1}} \beta_{i,t}^\delta.$$

Since  $\|\Lambda(\bar{\boldsymbol{\theta}} - \boldsymbol{\theta}^*)\|_{\Lambda^{-1}} = \|\bar{\boldsymbol{\theta}} - \boldsymbol{\theta}^*\|_{\Lambda}$ , we divide both sides by  $\|\bar{\boldsymbol{\theta}} - \boldsymbol{\theta}^*\|_{\Lambda}$ , and obtain

$$\|\bar{\boldsymbol{\theta}} - \boldsymbol{\theta}^*\|_{\Lambda} \leq \beta_{i,t}^\delta \quad \forall t \geq 0,$$

which holds with probability at least  $(1 - 2\delta_i)$ . Using the definition of the confidence sets  $\mathcal{C}_{i,t}^\delta$  in (6) and the result above, this concludes our proof.  $\square$

### B. Robust Obstacle Avoidance Constraints Implementation

We describe our implementation of obstacle avoidance constraints in the special case where all obstacles are spheres in  $\mathbb{R}^3$  and the system is a manipulator. Other types of constraints (e.g., linear constraints), obstacles (e.g., polyhedral and non-convex obstacles), as well as point-mass systems, are particular cases of the following derivations, as we discuss next.

Consider a function  $\mathbf{p} : \mathbb{R}^n \rightarrow \mathbb{R}^3$  mapping the state of the system (its configuration) to a point that should not intersect with obstacles (e.g., for a manipulator,  $\mathbf{p}$  is the end-effector position as a function of the joint angles. For a point-mass system,  $\mathbf{p}$  maps to the positional variables only).

<sup>7</sup> $\mathbb{P}((19) \cap (20)) = 1 - \mathbb{P}((19)^C \cup (20)^C)$ , where  $A^C$  denotes the negation of  $A$ . Then, by Boole's inequality,  $1 - \mathbb{P}((19)^C \cup (20)^C) \geq 1 - \mathbb{P}((19)^C) - \mathbb{P}((20)^C) = -1 + \mathbb{P}((19)) + \mathbb{P}((20))$ . Finally, using the lower bounds on the probabilities that (19) and (20) occur, we obtain  $\mathbb{P}((19) \cap (20)) \geq -1 + (1 - \delta_i) + (1 - \delta_i) = 1 - 2\delta_i$ .

Before treating the robust case under uncertainty, consider this constraint for a single state  $\mathbf{x} \in \mathbb{R}^n$ . Given a spherical obstacle  $\mathcal{O} = \{\bar{\mathbf{p}} \in \mathbb{R}^3 \mid \|\bar{\mathbf{p}} - \mathbf{p}_0\|_2 < r_o, \mathbf{p}_0 \in \mathbb{R}^3, r_o > 0\}$ , we define the obstacle avoidance constraint as  $\mathbf{p}(\mathbf{x}) \notin \mathcal{O}$ , which is equivalent to  $\|\mathbf{p}(\mathbf{x}) - \mathbf{p}_0\|_2 - r_o \geq 0$ . Defining  $d(\mathbf{x}) = \|\mathbf{p}(\mathbf{x}) - \mathbf{p}_0\|_2 - r_o$ , we observe that  $d(\mathbf{x}) \geq 0$  is a non-convex constraint. To tackle this type of constraints, sequential convex programming (SCP) consists of solving a sequence of convex programs where any non-convex constraint is linearized. Specifically, the linearization of this constraint at  $\mathbf{x}^j \in \mathbb{R}^n$  is

$$d(\mathbf{x}^j) + \left( \frac{\mathbf{p}(\mathbf{x}^j) - \mathbf{p}_0}{\|\mathbf{p}(\mathbf{x}^j) - \mathbf{p}_0\|_2} \right)^\top \left( \frac{\partial \mathbf{p}}{\partial \mathbf{x}}(\mathbf{x}^j) \right) (\mathbf{x} - \mathbf{x}^j) \geq 0,$$

where the term multiplying  $(\mathbf{x} - \mathbf{x}^j)$  corresponds to  $\frac{\partial d}{\partial \mathbf{x}}(\mathbf{x}^j)$ , and  $\frac{\partial \mathbf{p}}{\partial \mathbf{x}}(\mathbf{x}^j) \in \mathbb{R}^{3 \times 6}$  denotes the Jacobian of  $\mathbf{p}$  evaluated at  $\mathbf{x}^j$ . This constraint is linear in  $\mathbf{x}$  and can be handled by off-the-shelf convex optimization algorithms. Note that the case where  $\mathcal{O}$  is an arbitrary non-convex set can be handled similarly by replacing  $d(\mathbf{x})$  with a signed distance function, see [27].

Next, we treat the robust constraint  $\mathbf{p}(\mathbf{x}) \notin \mathcal{O} \forall \mathbf{x} \in \mathcal{X}$ , with  $\mathcal{X} \subset \mathbb{R}^6$  a reachable set. A conservative reformulation consists of defining an outer-bounding rectangular set  $\mathcal{D} = \{\mathbf{x} \in \mathbb{R}^6 \mid |x_i - \mu_i| \leq \delta_i, \boldsymbol{\mu} \in \mathbb{R}^6, \delta_i > 0\}$  such that  $\mathcal{X} \subseteq \mathcal{D}$ . In this work, as we use a sampling-based algorithm to approximate each reachable set,  $\mathcal{X}$  is finite, i.e.,  $\mathcal{X} = \{\mathbf{x}^j\}_{j=1}^M$ . Thus, we simply choose the nominal predicted state  $\boldsymbol{\mu}_k$  (see REACH-OCF) for the center  $\boldsymbol{\mu}$  of each rectangular set  $\mathcal{D}$ , and we choose  $\delta_i = \max_j |x_i^j - \mu_i|$  for its half-width.

Then, we define an outer-bounding ellipsoidal set  $\mathcal{E} = \{\mathbf{x} \in \mathbb{R}^n \mid (\mathbf{x} - \boldsymbol{\mu})^\top \mathbf{Q}^{-1}(\mathbf{x} - \boldsymbol{\mu}) \leq 1\}$ , where the center  $\boldsymbol{\mu}$  is the same as the center of the rectangular set  $\mathcal{D}$ , and  $\mathbf{Q} = n \cdot \text{diag}(\delta_i^2, i=1, \dots, n)$  is a diagonal positive definite matrix<sup>8</sup>. This construction guarantees that  $\mathcal{X} \subseteq \mathcal{D} \subseteq \mathcal{E}$ , so that  $\mathcal{E}$  outer-bounds  $\mathcal{X}$ . Finally, we use this set to reformulate the robust constraint  $d(\mathbf{x}) \geq 0 \forall \mathbf{x} \in \mathcal{X}$  as  $d(\boldsymbol{\mu}) - \sqrt{\mathbf{J}^\top \mathbf{Q} \mathbf{J}} \geq 0$ , where  $\mathbf{J} = \frac{\partial d}{\partial \mathbf{x}}(\boldsymbol{\mu})$ , and  $\boldsymbol{\mu}$  is the nominal state of the trajectory, see REACH-OCF. For a justification of this reformulation, refer to [22], [27], [52]. Note that this constraint is non-convex in  $\boldsymbol{\mu}$ , and also depends on the control trajectory  $\mathbf{u}$  due to the dependence on  $\mathbf{Q}$  (which depends on the sampled trajectory when performing reachability analysis). We iteratively linearize this last constraint within each SCP iteration to obtain a quadratic program which is efficiently solved using OSQP [64].

<sup>8</sup>Observe that  $\mathbf{p}$  typically only depends on positional and angular variables, so the entries of the last rows of  $\frac{\partial \mathbf{p}}{\partial \mathbf{x}}(\mathbf{x}^j)$  are zero. Thus, one can reduce conservatism by formulating a constraint with  $\mathbf{Q} = n_{\text{pos}} \cdot \text{diag}(\delta_i^2, i=1, \dots, n_{\text{pos}})$  instead, where  $n_{\text{pos}} < n$  (e.g., for a three-joint manipulator,  $n_{\text{pos}} = 3 < 6 = n$ ).



**Thomas Lew** is a Ph.D. candidate in Aeronautics and Astronautics at Stanford University. He received his BSc. degree in Microengineering from Ecole Polytechnique Federale de Lausanne in 2017 and his MSc. degree in Robotics from ETH Zurich in 2019. His research focuses on the intersection between optimization, control theory, and machine learning techniques for robotics and aerospace applications.



**Marco Pavone** is an Associate Professor of Aeronautics and Astronautics at Stanford University, where he is the Director of the Autonomous Systems Laboratory. Before joining Stanford, he was a Research Technologist within the Robotics Section at the NASA Jet Propulsion Laboratory. He received a Ph.D. degree in Aeronautics and Astronautics from the Massachusetts Institute of Technology in 2010. His main research interests are in the development of methodologies for the analysis, design, and control of autonomous systems, with an emphasis on self-driving cars, autonomous aerospace vehicles, and future mobility systems. He is a recipient of a number of awards, including a Presidential Early Career Award for Scientists and Engineers, an ONR YIP Award, an NSF CAREER Award, and a NASA Early Career Faculty Award. He was identified by the American Society for Engineering Education (ASEE) as one of America's 20 most highly promising investigators under the age of 40. He is currently serving as an Associate Editor for the IEEE Control Systems Magazine.



**Apoorva Sharma** is a PhD candidate in the Autonomous Systems Lab at Stanford University. He received an M.S. degree in Aeronautics and Astronautics from Stanford University in 2018, and a B.S. degree in Engineering from Harvey Mudd College in 2016. His research interests center around the application of machine learning models in control and sequential decision making applications, with a focus on Bayesian methods and quantifying uncertainty to enable safe application of machine learning systems in robot autonomy and decision making.



**James Harrison** is a Ph.D. candidate in the Autonomous Systems Lab at Stanford University. He received an M.S. degree from Stanford University in 2018 and a B.Eng. degree from McGill University in 2015, both in mechanical engineering. His research interests include few-shot, adaptive, and open-world learning, Bayesian deep learning, and applications in safe robot autonomy, decision-making, and control.



**Andrew Bylard** is a Ph.D. candidate in Aeronautics and Astronautics at Stanford University. He received a B.Eng. with a dual concentration in Mechanical Engineering and Electrical Engineering from Walla Walla University in 2014 and a M.Sc. in Aeronautics and Astronautics from Stanford University in 2016. Andrew's research interests include real-time trajectory planning and optimization and unconventional space robotics, including using gecko-inspired adhesives for microgravity manipulation and repurposing rollable extendable booms for long-reach mobile

manipulators in reduced gravity. He has been a lead developer at the Stanford Space Robotics Facility, where he designed robot test beds used to perform spacecraft contact dynamics experiments and develop autonomous space robotics capabilities under simulated frictionless, microgravity conditions.